Structure–properties relationship of the derivatives of carbazole and 1,8-naphthalimide: Effects of the substitution and the linking topology

ARTICLE *in* DYES AND PIGMENTS · MARCH 2015

Impact Factor: 3.97 · DOI: 10.1016/j.dyepig.2014.11.013

8 AUTHORS, INCLUDING:

D. Gudeika
Kaunas University of Technology
21 PUBLICATIONS **69** CITATIONS
SEE PROFILE

G. Juška
Vilnius University
116 PUBLICATIONS **2,456** CITATIONS
SEE PROFILE

Arunas Miasojedovas
Vilnius University
16 PUBLICATIONS **159** CITATIONS
SEE PROFILE

Saulius Jursenas
Vilnius University
146 PUBLICATIONS **1,109** CITATIONS
SEE PROFILE

Dyes and Pigments 114 (2015) 239–252

Contents lists available at ScienceDirect

Dyes and Pigments

journal homepage: www.elsevier.com/locate/dyepig

Structure-properties relationship of the derivatives of carbazole and 1,8-naphthalimide: Effects of the substitution and the linking topology

Dalius Gudeika [a], Juozas Vidas Grazulevicius [a, *], Dmytro Volyniuk [a], Rita Butkute [a], Gytis Juska [b], Arunas Miasojedovas [c], Alytis Gruodis [d], Saulius Jursenas [c]

[a] Department of Polymer Chemistry and Technology, Kaunas University of Technology, Radvilenu pl. 19, LT-50254 Kaunas, Lithuania
[b] Department of Solid State Electronics, Vilnius University, Sauletekio, aleja 9, LT-10222 Vilnius, Lithuania
[c] Departmentof General Physics and Spectroscopy, Vilnius University, Sauletekio, aleja 9, LT-10222 Vilnius, Lithuania
[d] Institute of Applied Research, Vilnius University, Sauletekio aleja 9, LT-10222 Vilnius, Lithuania

ARTICLE INFO

Article history:
Received 19 August 2014
Received in revised form
12 November 2014
Accepted 14 November 2014
Available online 21 November 2014

Keywords:
Palladium-catalyzed
Molecular glass
Ionization potential
Photophysical properties
Intramolecular charge-transfer
Intramolecular twisting

ABSTRACT

Nine compounds having electron-accepting 1,8-naphthalimide and electron-donating carbazole moieties were synthesized employing palladium-catalyzed C–N and C–C coupling reactions and characterized by the thermal methods, absorption and emission spectrometry, electrochemical and photoelectrical tools. The synthesized compounds possess high thermal stability with the 5% weight loss temperatures being in the range of 351–476 °C. Most of the synthesized compounds are capable of glass formation with glass transition temperatures ranging from 30 to 87 °C. The cyclic voltammetry measurements showed that the solid state ionization potentials values of the carbazole and 1,8-naphthalimide derivatives range from 5.46 eV to 5.76 eV and the electron affinities values range from −3.04 eV to −2.92 eV. Dilute solutions of the 3- and 3,6-naphthalimide-substituted derivatives of carbazole in polar solvents were found to emit in the green region with quantum yields ranging from 0.66 to 0.83, while in the solid state fluorescence quantum yields were found to be in the range of 0.01–0.45. ((E)-9-(((*N*-(2-ethylhexyl)-1,8-naphthalimide)-4-yl)ethenyl)-9*H*-carbazole) exhibited efficient fluorescence in the solid state with quantum yield as high as 0.45. The effects of the linking topology of the chromophores and of the incorporated alkyl substituents on the thermal, optical, and photoelectrical properties of the synthesized donor-acceptor compounds are analyzed. The impact of the ground state intramolecular twisting of the carbazole and naphthalimide moieties induced by the substituents resulting in significant variation in the rates of radiative and nonradiative excitation deactivation is revealed.

1. Introduction

Conjugated compounds containing both donor and acceptor moieties have been extensively synthesized and studied because of their potential applications in electronics and optoelectronics [1–3]. The unique structure of donor-acceptor molecules allows their optical and electrochemical properties to be tuned finely over a wide range by appropriate chemical modification of the donor and acceptor moieties [4]. The further progress in the design and synthesis of the compounds containing both donor and acceptor moieties depend to the great extent on the understanding the structure-property relationship of such compounds.

Derivatives of 1,8-naphthalimide are widely used for various applications [5,6]. They were utilized in such fields as colouration and brightening of polymers [7], as laser active media [8,9], fluorescent markers in biology [10], anticancer agents [11], analgesics in medicine [12], fluorescence switchers and sensors [13–16], as electron-transporting and emitting materials in light emitting diodes [17–19]. They were also used in liquid crystal displays [20] and as ion probes [21–23]. Derivatives of 1,8-naphthalimide derivatives generally have high electron affinity due to the existence of an electron-deficient centre [24] and display good electron-transporting or hole-blocking capabilities.1,8-Naphthalimide moiety can be easily functionalized [25]. By introducing different electron-donating substituents at C-4 position of 1,8-naphthalimide moiety the emission color of the compounds can be readily tuned from near infrared to pure blue [26–29].

* Corresponding author. Tel.: +370 37 300193; fax: +370 37 300152.
E-mail address: juozas.grazulevicius@ktu.lt (J.V. Grazulevicius).

http://dx.doi.org/10.1016/j.dyepig.2014.11.013
0143-7208/

Carbazole-based compounds are known for their intense blue luminescence and electroluminescence [30,31]. Carbazole derivatives are prefereable due to their rigid plane and good hole-transporting properties [32]. Carbazole derivatives, consisting of large planar aromatic systems possess enhanced thermal stability [33–35]. Furthermore, carbazole moiety can easily be functionalized at its C-3 and C-6 [36], as well as at C-2 and C-7 [37] or *N*-positions [38], allowing the fine-tuning of the electro-optical properties of the molecules [39,40]. Many reported carbazole-based materials are equipped with substituents at its C-3 and C-6-positions to enhance morphological and electrochemical stability [41]. Recently, a series of carbazole derivatives with donor-acceptor structures was reported as efficient emitting materials for organic devices [42–44]. Such carbazole derivatives have a great potential for the application as host materials in organic light emitting diodes [45], therefore the molecular design and synthesis of new carbazole derivatives with donor-acceptor structure need to be further developed by the structural modification in order to improve the properties and to establish the relationship between structures and properties.

In this paper we present the synthesis by stepwise palladium-catalyzed C–N and C–C coupling reactions of a series of acceptor-donor-(acceptor) compounds having electron-accepting 1,8-naphthalimide moieties linked to electron-donating carbazole species functionalized at three different positions (C-3, C-6 and N-9). One of the aims of this work was to explore the effects of the linking topology of the chromophores and the nature of alkyl substituents introduced at the carbazole nitrogen on the thermal, optical, photophysical and photoelectrical properties of the compounds. Basing on the results of the density-functional modeling and detailed studies of the optical and photophysical properties of the compounds embedded in various surrounding media the impact of the conformational changes of the singly bonded carbazole-naphthalimide systems is elucidated and its impact on the nonradiative and radiative excited state deactivation is discussed.

2. Experimental methods

2.1. Instrumentation

Nuclear magnetic resonance (^{1}H NMR and ^{13}C NMR) spectra were obtained using a Varrian Unity Inova (300 MHz (^{1}H), 75.4 MHz (^{13}C)). All the data are given as chemical shifts in δ (ppm), multiplicity, integration downfield from $(CH_3)_4Si$. Mass (MS) spectra were obtained on a Waters ZQ 2000 (Milford, USA). Elemental analysis was performed with an Exeter Analytical CE-440 Elemental Analyser. Infrared (IR) spectra were recorded using Perkin Elmer Spectrum GX spectrometer. DSC measurements were carried out using a Perkin–Elmer DSC-7 series thermal analyzer at a heating rate 10 °C/min under nitrogen flow. TGA measurements were performed on a METTLER TOLEDO TGA/SDTA 851^e. Melting point (m.p.) of the material was determined using Electrothermal Mel-Temp apparatus. Ionization potentials (IP_{EP}) were established by electron photoemission technique in air [46]. The samples for the measurements were prepared by dissolving the compounds in THF and by coating onAl plates precoated with ~0.5 μm thick methylmethacrylate and methacrylic acid copolymer adhesive layer [47]. Electrochemical investigation was carried out using Bio-Logic SAS and a micro-AUTOLAB Type III potentiostat-galvanostat. The solutions of the synthesized compounds with the concentration of 10^{-5} M were used for cyclic voltamperometry (CV) measurements. The experiments were calibrated with the standard ferrocene/ferrocenium redox system [48].

Charge drift mobility measurements were performed using charge extraction by linearly increasing voltage (CELIV) method [49,50]. For the CELIV measurements the samples in configuration ITO/compound/Al with the thickness of layers organic compound of 100–200 nm and an active area of 7 mm^2 were prepared. The layers from 10 mg/mL THF solutions of the compounds were spin coated onto glass/ITO substrates at 1000 rpm. Glass/ITO substrates were sonicated in acetone, deionized water, and isopropanol for 10 min before use. Al electrode of 60 nm of was thermally evaporated at 10 Å/s at a pressure below $5\cdot10^{-5}$ mbar using a mask, to obtain three top contact pixels. The light pulse was used to photogenerate the charge carriers by exciting layers of compounds through the ITO layer. The charge carriers were generated by illumination with pulses of Nd:YAG laser (pulse duration was 25 ps, wavelength 355 nm). The experimental setup consisted of a delay generator Tektronix AFG 3011 and a digital storage oscilloscope Tektronix DPO 4032.

Absorption spectra of the dilute solutions of the investigated compounds were recorded by UV-Vis-NIR spectrophotometer Lambda 950 (Perkin Elmer). Fluorescence of dilute solutions, compounds embedded in polystyrene (PS) matrix and of the neat films was excited at a 365 and 420 nm wavelengths from 150 W xenon arc lamp light source passed through a monochromator and measured using back-thinned CCD spectrophotometer PMA-11 (Hamamatsu). For these measurements, the dilute solutions of the investigated compounds were prepared by dissolving them in a spectral grade solvent at 10^{-6} M concentration. The PS films with the dispersed compounds with concentration of 1 wt% were prepared by mixing the dissolved compounds and PS in THF and casting the solutions on quartz substrates in an ambient air. The drop-casting from THF solutions (1×10^{-3} M) was also employed to prepare the neat films of the compounds. Fluorescence quantum yields (QY) of the solutions were estimated by using integrated sphere method [51]. Integrating sphere (Sphere Optics) coupled to the CCD spectrometer via optical fiber was also employed to measure η of the neat films. Fluorescence transients of the samples were measured using a time-correlated single photon counting system PicoHarp 300 (PicoQuant) utilizing semiconductor diode laser (repetition rate 1 MHz, pulse duration 70 ps, emission wavelength 375 nm) as an excitation source.

2.2. Materials

4-Bromo-1,8-naphthalic anhydride and 2-ethylhexylamine were purchased from TCI. Tri-*o*-tolylphosphine and 9*H*-carbazole were purchased from Fluka and Reakhim respectively. 1-Iodomethane, 1-bromobutane, 2-ethylhexylbromide, *n*-BuLi (2.5 mol L^{-1} in hexane), 2-isopropoxy-4,4,5,5-tetramethyl-1,3,2-dioxaborolane, bis(triphenylphosphine)palladium(II) dichloride ($Pd(PPh_3)_2Cl_2$) and *N*-bromosuccinimide (NBS), palladium acetate(II) ($Pd(OAc)_2$), 18-crown-6, *N*-vinylcarbazole, triethylamine, copper were obtained from Aldrich. The solvent, i.e. dimethylformamide (DMF, Lachema) was dried by distillation over CaH_2. THF was dried and distilled over sodium and benzophenone. Dichloromethane (POCH), ethyl acetate and *n*-Hexane (Penta) were purified and dried using the standard procedures [52]. All other reagents and solvents were used as supplied.

3,6-Dibromocarbazole (**1a**) [53] (m.p. 207–208 °C, lit. [54] m.p. 209–210 °C), 3-bromocarbazole (**1b**) [55] (m.p. 192–193 °C, lit. [54] m.p. 197–198 °C), 3,6-dibromo-9-methyl-9*H*-carbazole (**2a**) [56] (m.p. 136–137 °C, lit. [56] m.p. 141 °C), 3,6-dibromo-*N*-butylcarbazole (**2b**) [57] (m.p. 71–72 °C, lit. [58] m.p. = 74–75 °C), 3,6-dibromo-9-(2-ethylhexyl)carbazole (**2c**) [59] (colorless oil), 3-bromo-9-methylcarbazole (**2d**) [53] (m.p. 74–75, lit. [56] m.p. = 78–79 °C), 3-bromo-9-butylcarbazole (**2e**) [60] (colorless

oil), 3-bromo-9-(2-ethylhexyl)carbazole (**2f**) [61] (colorless oil), 9-methyl-3,6-(4,4,5,5-tetramethyl[1,3,2]dioxaborolan-2-yl)-9*H*-carbazole (**3a**) [62] (m.p. 249–250 °C, lit. [62] m.p. 257–259 °C), 9-butyl-3,6-(4,4,5,5-tetramethyl[1,3,2]dioxaborolan-2-yl)-9*H*-carbazole (**3b**) [63] (colorless oil), 9-(2-ethylhexyl)-3,6-(4,4,5,5-tetramethyl[1,3,2]dioxaborolan-2-yl)-9*H*-carbazole (**3c**) [64] (colorless oil), 9-methyl-3-(4,4,5,5-tetramethyl[1,3,2]dioxaborolan-2-yl)-9*H*-carbazole (**3d**) [59] (m.p. 142–144 °C, lit. [62] m.p 147–149 °C), 9-butyl-3-(4,4,5,5-tetramethyl[1,3,2]dioxaborolan-2-yl)-9*H*-carbazole (**3e**) [65] (colorless oil), 9-(2-ethylhexyl)-3-(4,4,5,5-tetramethyl[1,3,2]dioxaborolan-2-yl)-9*H*-carbazole (**3f**) [61] (colorless oil), 4-bromo-*N*-(2-ethylhexyl)-1,8-naphthalimide (**4**) [66] and 3,6-di-*tert*-butyl-9*H*-carbazole [67] (m.p. 221–222 °C, lit. [68] m.p. 228 °C) were prepared according to the published procedures.

2.3. Synthesis

2.3.1. 3,6-((Di(N-(2-ethylhexyl)-1,8-naphthalimide)-4-yl)-9-metyl-9H-carbazole (5)

4-Bromo-*N*-(2-ethylhexyl)-1,8-naphthalimide (**4**) (0.5 g, 1.29 mmol) and 15 mL of dry THF and aqueous K_2CO_3 solution (0.81 g, 5.85 mmol) in 2 mL H_2O were added via a syringe under nitrogen to a three-necked round-bottomed flask (50 mL) equipped with a magnetic stirrer, a reflux condenser and a nitrogen input tube. 9-Methyl-3,6-(4,4,5,5-tetramethyl[1,3,2]dioxaborolan-2-yl)-9*H*-carbazole (**3a**) (0.25 g, 0.59 mmol) and $Pd(PPh_3)_2Cl_2$ (0.02 g, 0.02 mmol) were successively added and the reaction mixture was refluxed at 80 °C for 24 h under nitrogen atmosphere. After cooling down to the room temperature methylene chloride (200 mL) was added to the reaction mixture. Then it was washed three times with distilled water, and dried with anhydrous magnesium sulfate. The solution was filtered and concentrated. The crude product was purified by column chromatography on silica gel with ethyl acetate and hexane (1:9, *V*:*V*) as eluent and crystallized from the eluent mixture of solvents to give **5** as yellow crystals. Yield: 66% (0.31 g), m.p. 147–148 °C; ^{1}H NMR spectrum (300 MHz, $CDCl_3$, δ, ppm): 8.71 (s, 1H, $-H_{Naphthalene}$), 8.69 (s, 1H, $-H_{Naphthalene}$), 8.68 (d, 1H, J = 1.1 Hz, $-H_{Naphthalene}$), 8.65 (d, 1H, J = 1.1 Hz, $-H_{Naphthalene}$), 8.42 (d, 1H, J = 1.1 Hz, $-H_{Naphthalene}$), 8.39 (d, 1H, J = 1.1 Hz, $-H_{Naphthalene}$), 8.33–8.28 (m, 2H, $-H_{Naphthalene}$), 7.85 (d, 2H, J = 7.6 Hz, $-H_{Naphthalene}$), 7.75 (s, 2H, $-H_{Naphthalene}$, $-H_{Carbazole}$), 7.72 (t, 3H, J = 1.6 Hz, $-H_{Carbazole}$), 7.70 (s, 2H, $-H_{Carbazole}$), 4.22–4.16 (m, 4H, $-N(CH_2)_2$, $-H_{aliphatic}$), 4.10 (s, 3H, $-NCH_2CH_2CH_2CH_3$), 2.05–1.97 (m, 2H, 2 × CH, $-H_{aliphatic}$), 1.47–1.32 (m, 16H, 8 × CH_2, $-H_{aliphatic}$), 1.00–0.90 (m, 12H, 4 × CH_3, $-H_{aliphatic}$). ^{13}C NMR spectrum (75.4 MHz, $CDCl_3$, δ, ppm): 164.9, 164.8, 147.8, 141.6, 133.1, 131.4, 131.1, 130.7, 130.3, 129.1, 128.5, 127.0, 123.2, 123.1, 122.2, 121.6, 109.2, 44.4, 38.2, 31.0, 29.8, 29.0, 24.3, 23.3, 14.4, 10.9. IR, (in KBr), cm^{-1}: 3070 ν (CH_{ar}); 2955, 2924, 2856 ν ($CH_{aliphatic}$); 1700 ν (C=$O_{anhydride}$); 1654, 1586, 1510 ν (C=C_{ar}); 1352, 1279 ν (C–N); 782, 754, 621 γ (CH_{ar}). MS ($APCI^+$, 20 V), *m*/*z*: 812 ($[M+H]^+$). Anal. Calcd. for $C_{54}H_{57}N_3O_4$: C, 79.87; H, 7.08, N, 5.17; O, 7.88%; found C 79.92, H 7.03, N 5.15%.

2.3.2. 3,6-Di((N-(2-ethylhexyl)-1,8-naphthalimide)-4-yl)-9-butyl-9H-carbazole (6)

The synthesis of **6** was carried out as described for **5** using 4-bromo-*N*-(2-ethylhexyl)-1,8-naphthalimide (**4**) (0.5 g, 1.29 mmol), 9-butyl-3,6-(4,4,5,5-tetramethyl[1,3,2]dioxaborolan-2-yl)-9*H*-carbazole (**3b**) (0.28 g, 0.59 mmol), $Pd(PPh_3)_2Cl_2$ (0.02 g, 0.02 mmol), K_2CO_3 (0.81 g, 5.85 mmol). The crude product was purified by column chromatography on silica gel with ethyl acetate and hexane (1:8, *V*:*V*) as an eluent and crystallized from the eluent mixture of solvents to give **6** as yellow crystals. Yield: 68% (0.34 g), m.p. = 177–178 °C; ^{1}H NMR spectrum (300 MHz, $CDCl_3$, δ, ppm): 8.72 (s, 1H, $-H_{Naphthalene}$), 8.69 (s, 1H, $-H_{Naphthalene}$), 8.68 (d, 1H, J = 1.2 Hz, $-H_{Naphthalene}$), 8.66 (d, 1H, J = 1.1 Hz, $-H_{Naphthalene}$), 8.45 (d, 1H, J = 1.2 Hz, $-H_{Naphthalene}$), 8.42 (d, 1H, J = 1.2 Hz, $-H_{Naphthalene}$), 8.30–8.29 (m, 2H, $-H_{Naphthalene}$), 7.86 (d, 2H, J = 7.6 Hz, $-H_{Naphthalene}$), 7.76 (s, 1H, $-H_{Naphthalene}$), 7.73 (d, 2H, J = 1.2 Hz, $-H_{Carbazole}$), 7.72–7.68 (m, 4H, $-H_{Carbazole}$), 4.55–4.52 (m, 2H, $-NCH_2CH_2CH_2CH_3$, $-H_{aliphatic}$), 4.23–4.15 (m, 4H, $-N(CH_2)_2$, $-H_{aliphatic}$), 2.06–2.01 (m, 2H, 2 × CH, $-H_{aliphatic}$), 1.91–1.86 (m, 2H, $-NCH_2CH_2CH_2CH_3$, $-H_{aliphatic}$), 1.48–1.30 (m, 18H, 9 × CH_2, $-H_{aliphatic}$), 1.02–0.86 (m, 15H, 5 × CH_3, $-H_{aliphatic}$). ^{13}C NMR spectrum (75.4 MHz, $CDCl_3$, δ, ppm): 164.7, 164.6, 148.7, 142.7, 133.4, 132.2, 131.1, 130.8, 129.3, 129.0, 128.7, 127.2, 124.2, 123.4, 122.8, 121.6, 110.1, 61.0, 45.4, 37.8, 36.7, 35.9, 31.0, 28.7, 27.1, 25.7, 23.3, 15.0, 11.7. IR, (in KBr), cm^{-1}: 3072 ν (CH_{ar}); 2958, 2926, 2857 ν ($CH_{aliphatic}$); 1699 ν (C=$O_{anhydride}$); 1656, 1588, 1512, 1463 ν (C=C_{ar}); 1354, 1277 ν (C–N); 783, 759, 623 γ (CH_{ar}). MS ($APCI^+$, 20 V), *m*/*z*: 854 ($[M+H]^+$). Anal. Calcd. for $C_{57}H_{63}N_3O_4$: C, 80.15; H, 7.43, N, 4.92; O, 7.49%; found C 80.21, H 7.40, N 5.98%.

2.3.3. 3,6-((Di(N-(2-ethylhexyl)-1,8-naphthalimide)-4-yl)-9-(2-ethylhexyl)-9H-carbazole (7)

The synthesis of **7** was carried out as described for **5** using 4-bromo-*N*-(2-ethylhexyl)-1,8-naphthalimide (**4**) (0.5 g, 1.29 mmol), 9-(2-ethylhexyl)-3,6-(4,4,5,5-tetramethyl[1,3,2]dioxaborolan-2-yl)-9*H*-carbazole (**3c**) (0.32 g, 0.59 mmol), $(PPh_3)_2Cl_2$ (0.02 g, 0.02 mmol), K_2CO_3 (0.81 g, 5.85 mmol). The crude product was purified by column chromatography on silica gel with ethyl acetate and hexane (1:10, *V*:*V*) as an eluent and crystallized from the eluent mixture of solvents to give **7** as yellow crystals. Yield: 63% (0.35 g), m.p. 102–103 °C; ^{1}H NMR spectrum (300 MHz, $CDCl_3$, δ, ppm): 8.73 (s, 1H, $-H_{Naphthalene}$), 8.70 (d, 2H, J = 1.5 Hz, $-H_{Naphthalene}$), 8.68 (d, 1H, J = 1.2 Hz, $-H_{Naphthalene}$), 8.44 (d, 1H, J = 1.2 Hz, $-H_{Naphthalene}$), 8.41 (d, 1H, J = 1.2 Hz, $-H_{Naphthalene}$), 8.22 (d, 1H, J = 1.6 Hz, $-H_{Naphthalene}$), 7.85 (s, 2H, J = 7.6 Hz, $-H_{Naphthalene}$), 7.77 (s, 1H, $-H_{Naphthalene}$), 7.75 (d, 2H, J = 1.2 Hz, $-H_{Carbazole}$), 7.68 (d, J = 1.8 Hz, $-H_{Carbazole}$), 7.66–7.64 (m, 1H, $-H_{Carbazole}$), 7.62–7.56 (m, 3H, $-H_{Carbazole}$), 4.25–4.19 (m, 6H, $-N(CH_2)_3$, $-H_{aliphatic}$), 2.06–1.98 (m, 2H, 2 × CH, $-H_{aliphatic}$), 1.49–1.32 (m, 25H, 12 × CH_2, –CH, $-H_{aliphatic}$), 1.03–0.91 (m, 18H, 6 × CH_3, $-H_{aliphatic}$). ^{13}C NMR spectrum (75.4 MHz, $CDCl_3$, δ, ppm): 163.6, 161.8, 148.7, 142.5, 134.2, 132.3, 131.2, 130.6, 130.3, 129.7, 128.4, 127.1, 124.7, 123.1, 122.2, 121.6, 111.7, 63.5, 43.3, 38.2, 37.8, 36.3, 32.2, 29.8, 26.1, 24.3, 23.3, 14.3, 11.9. IR, (in KBr), cm^{-1}: 3071 ν (CH_{ar}); 2958, 2925, 2855 ν ($CH_{aliphatic}$); 1698 ν (C=$O_{anhydride}$); 1655, 1578, 1522, 1462 ν (C=C_{ar}); 1351, 1278 ν (C–N); 782, 759, 622 γ (CH_{ar}). MS ($APCI^+$, 20 V), *m*/*z*: 910 ($[M+H]^+$). Anal. Calcd. for $C_{61}H_{71}N_3O_4$: C, 80.49; H, 7.86, N, 4.62; O, 7.03%; found C 80.45, H 7.82, N 7.08%.

2.3.4. 3-((N-(2-ethylhexyl)-1,8-naphthalimide)-4-yl)-9-metyl-9H-carbazole (8)

The synthesis of **8** was carried out as described for **5** using 4-bromo-*N*-(2-ethylhexyl)-1,8-naphthalimide (**4**) (0.5 g, 1.29 mmol), 9-methyl-3-(4,4,5,5-tetramethyl[1,3,2]dioxaborolan-2-yl)-9*H*-carbazole (**3d**), (0.47 g, 1.55 mmol), $(PPh_3)_2Cl_2$ (0.02 g, 0.02 mmol), K_2CO_3 (0.81 g, 5.85 mmol). The crude product was purified by column chromatography on silica gel with ethyl acetate and hexane (1:8, *V*:*V*) as an eluent and crystallized from the eluent mixture of solvents to give **8** as yellow crystals. Yield: 65% (0.42 g), m.p. 122–123 °C; ^{1}H NMR spectrum (300 MHz, $CDCl_3$, δ, ppm): 8.71 (d, 1H, J = 7.6 Hz, $-H_{Naphthalene}$), 8.68 (dd, 1H, J_1 = 1.2 Hz, J_2 = 7.3 Hz, $-H_{Naphthalene}$), 8.43 (dd, 1H, J_1 = 1.2 Hz, J_2 = 8.6 Hz, $-H_{Naphthalene}$), 8.27 (d, 1H, J = 2.3 Hz, $-H_{Naphthalene}$), 8.16 (d, 1H, J = 7.8 Hz, $-H_{Naphthalene}$), 7.86 (d, 1H, J = 7.6 Hz, $-H_{Carbazole}$), 7.73 (dd, 1H, J_1 = 7.3 Hz, J_2 = 8.5 Hz, $-H_{Carbazole}$), 7.66 (dd, 1H, J_1 = 1.7 Hz,

J_2 = 8.4 Hz, $-H_{Carbazole}$), 7.63–7.49 (m, 3H, $-H_{Carbazole}$), 7.33 (dd, 1H, J_1 = 1.5 Hz, J_2 = 7.4 Hz, $-H_{Carbazole}$), 4.27–4.15 (m, 2H, $-NCH_2$, $-H_{aliphatic}$), 3.99 (s, 3H, $-NC\underline{H}_3$), 2.07–2.00 (m, 1H, CH, $-H_{aliphatic}$), 1.51–1.29 (m, 8H, 4 × CH_2, $-H_{aliphatic}$), 1.04–0.90 (m, 6H, 2 × CH_3, $-H_{aliphatic}$). ^{13}C NMR spectrum (75.4 MHz, $CDCl_3$, δ, ppm): 164.9, 148.2, 141.7, 133.6, 131.4, 131.1, 130.7, 129.7, 129.1, 128.5, 127.9, 126.9, 126.6, 123.3, 123.1, 122.7, 122.1, 121.4, 120.7, 119.6, 109.0, 108.8, 100.2, 44.4, 38.2, 31.0, 29.5, 29.0, 24.2, 23.3, 14.4, 10.9. IR, (in KBr), cm^{-1}: 3070 ν (CH_{ar}); 2957, 2923, 2851 ν ($CH_{aliphatic}$); 1703 ν ($C{=}O_{anhydride}$); 1648, 1569, 1511 ν ($C{=}C_{ar}$); 1354, 1277 ν (C–N); 782, 756, 622 γ (CH_{ar}). MS ($APCI^+$, 20 V), *m*/*z*: 505 ($[M + H]^+$). Anal. Calcd. for $C_{34}H_{36}N_2O_2$: C, 80.92; H, 7.19, N, 5.55; O, 6.34%; found C 80.85, H 7.15, N 5.58%.

2.3.5. 3-((N-(2-ethylhexyl)-1,8-naphthalimide)-4-yl)-9-butyl-9H-carbazole (**9**)

The synthesis of **9** was carried out as described for **5** using 4-bromo-*N*-(2-ethylhexyl)-1,8-naphthalimide (**4**) (0.5 g, 1.29 mmol), 9-butyl-3-(4,4,5,5-tetramethyl[1,3,2]dioxaborolan-2-yl)-9*H*-carbazole (**3e**) (0.54 g, 1.55 mmol), $(PPh_3)_2Cl_2$ (0.02 g, 0.02 mmol), K_2CO_3 (0.81 g, 5.85 mmol). The crude product was purified by column chromatography on silica gel with ethyl acetate and hexane (1:8, *V*:*V*) as an eluent and crystallized from the eluent mixture of solventsto give **9** as yellow crystals. Yield: 68% (0.48 g), m.p. = 115–116 °C; ^{1}H NMR spectrum (300 MHz, $CDCl_3$, δ, ppm): 8.73 (s, 1H, $-H_{Naphthalene}$), 8.71 (s, 1H, $-H_{Naphthalene}$), 8.69 (dd, 1H, J_1 = 1.1 Hz, J_2 = 7.3 Hz, $-H_{Naphthalene}$), 8.46 (dd, 1H, J_1 = 1.1 Hz, J_2 = 8.5 Hz, $-H_{Naphthalene}$), 8.28 (dd, 1H, J = 1.3 Hz, $-H_{Naphthalene}$), 8.16 (dd, 1H, J = 7.8 Hz, $-H_{Carbazole}$), 7.87 (d, 1H, J = 7.6 Hz, $-H_{Carbazole}$), 7.74 (dd, 1H, J_1 = 7.3 Hz, J_2 = 8.5 Hz, $-H_{Carbazole}$), 7.67–7.61 (m, 2H, $-H_{Carbazole}$), 7.60–7.52 (m, 2H, $-H_{Carbazole}$), 4.48–4.41 (m, 2H, $-NC\underline{H}_2CH_2CH_2CH_3$, $-H_{aliphatic}$), 4.26–4.17 (m, 4H, $-N(CH_2)_2$, $-H_{aliphatic}$), 2.01–1.96 (m, 1H, CH, $-H_{aliphatic}$), 1.57–1.24 (m, 12H, 6 × CH_2, $-H_{aliphatic}$), 1.09–0.87 (m, 9H, 3 × CH_3, $-H_{aliphatic}$). ^{13}C NMR spectrum (75.4 MHz, $CDCl_3$, δ, ppm): 163.9, 147.2, 140.7, 135.3, 132.0, 131.1, 130.7, 129.7, 129.5, 128.5, 127.8, 126.4, 126.2, 123.2, 123.1, 122.6, 122.5, 121.3, 120.7, 119.5, 109.0, 108.7, 107.2, 62.1, 43.4, 39.2, 35.2, 31.1, 29.9, 29.1, 24.2, 23.3, 15.4, 13.5, 10.8. IR, (in KBr), cm^{-1}: 3069 ν (CH_{ar}); 2954, 2924, 2838 ν ($CH_{aliphatic}$); 1701 ν ($C{=}O_{anhydride}$); 1656, 1577, 1523, 1466 ν ($C{=}C_{ar}$); 1357, 1267 ν (C–N); 789, 761, 619 γ (CH_{ar}). MS ($APCI^+$, 20 V), *m*/*z*: 547 ($[M+H]^+$). Anal. Calcd. for $C_{37}H_{42}N_2O_2$: C, 81.28; H, 7.74, N, 5.12; O, 5.85%; found C 81.33, H 7.68, N 5.88%.

2.3.6. 3-((N-(2-ethylhexyl)-1,8-naphthalimide)-4-yl)-9-(2-ethylhexyl)-9H-carbazole (**10**)

The synthesis of **10** was carried out as described for **5** using 4-bromo-*N*-(2-ethylhexyl)-1,8-naphthalimide (**4**) (0.5 g, 1.29 mmol), 9-(2-ethylhexyl)-3-(4,4,5,5-tetramethyl[1,3,2]dioxaborolan-2-yl)-9*H*-carbazole (**3f**) (0.63 g, 1.55 mmol), $(PPh_3)_2Cl_2$ (0.02 g, 0.02 mmol), K_2CO_3 (0.81 g, 5.85 mmol). The crude product was purified by column chromatography on silica gel with ethyl acetate and hexane (1:9, *V*:*V*) as an eluent and crystallized from the eluent mixture of solvents to give **10** as yellow crystals. Yield: 71% (0.55 g), m.p. 108–109 °C; ^{1}H NMR spectrum (300 MHz, $CDCl_3$, δ, ppm): 8.72 (d, 1H, J = 7.5 Hz, $-H_{Naphthalene}$), 8.69 (dd, 1H, J_1 = 1.2 Hz, J_2 = 3.4 Hz, $-H_{Naphthalene}$), 8.46 (dd, 1H, J_1 = 1.2 Hz, J_2 = 8.5 Hz, $-H_{Naphthalene}$), 8.27 (d, 1H, J = 2.2 Hz, $-H_{Naphthalene}$), 8.16 (d, 1H, J = 7.7 Hz, $-H_{Naphthalene}$), 8.08 (d, 1H, J = 7.9 Hz, $-H_{Carbazole}$), 7.87 (dd, 1H, J_1 = 1.9 Hz, J_2 = 7.4 Hz, $-H_{Carbazole}$), 7.74 (dd, 1H, J_1 = 7.3 Hz, J_2 = 8.5 Hz, $-H_{Carbazole}$), 7.64–7.51 (m, 3H, $-H_{Carbazole}$), 7.32 (dd, 1H, J_1 = 1.2 Hz, J_2 = 6.8 Hz, $-H_{Carbazole}$), 4.25–4.18 (m, 2H, $-NCH_2$, $-H_{aliphatic}$), 4.17–4.11 (m, 2H, $-NCH_2$, $-H_{aliphatic}$), 2.22–2.14 (m, 1H, CH, $-H_{aliphatic}$), 2.04–1.96 (m, 1H, CH, $-H_{aliphatic}$), 1.50–1.30 (m, 16H, 8 × CH_2, $-H_{aliphatic}$), 1.03–0.89 (m, 12H, 4 × CH_3, $-H_{aliphatic}$). ^{13}C NMR spectrum (75.4 MHz, $CDCl_3$, δ, ppm): 162.9, 14.2, 140.7, 134.3, 131.3, 131.1, 130.7, 129.7, 129.1, 128.5, 127.9, 126.9, 126.5, 123.2, 123.1, 122.7, 122.2, 121.4, 120.6, 119.7, 109.1, 108.9, 102.2, 63.1, 46.4, 38.2, 35.8, 31.0, 29.5, 29.1, 26.6, 24.2, 23.3, 14.3, 10.9. IR, (in KBr), cm^{-1}: 3072 ν (CH_{ar}); 2958, 2926, 2847 ν ($CH_{aliphatic}$); 1699 ν ($C{=}O_{anhydride}$); 1652, 1588, 1512, 1453 ν ($C{=}C_{ar}$); 1357, 1276 ν (C–N); 783, 759, 621 γ (CH_{ar}). MS ($APCI^+$, 20 V), *m*/*z*: 603 ($[M+H]^+$). Anal. Calcd. for $C_{41}H_{50}N_2O_2$: C, 81.69; H, 8.36, N, 4.65; O, 5.31%; found C 81.63, H 8.40, N 4.58%.

2.3.7. 9-((N-(2-ethylhexyl)-1,8-naphthalimide)-4-yl)-9H-carbazole (**11**)

4-Bromo-*N*-(2-ethylhexyl)-1,8-naphthalimide (**4**) (0.5 g, 1.29 mmol), copper powder (0.32 g, 5.15 mmol), 18-crown-6 (0.06 g, 0.26 mmol), K_2CO_3 (1.42 g, 10.31 mmol), 9*H*-carbazole (0.94 g, 5.14 mmol) and *o*-dichlorobenzene (15 mL) were placed into a round-bottom flask and vigorously stirred at 180 °C for 24 h under nitrogen. When the reaction was finished, the inorganic components were removed by filtration. The solvent was removed by distillation under reduced pressure. The crude product was purified by column chromatography using the mixture of ethyl acetate and hexane (1:9, *V*:*V*) as an eluent and crystallized from the eluent mixture of solvents to obtain **11** as yellow crystals. Yield: 58% (0.36 g), m.p. 110–111 °C; ^{1}H NMR spectrum (300 MHz, CDCl3, δ, ppm): 8.83 (d, 1H, J = 7.7 Hz, $-H_{Naphthalene}$), 8.72 (d, 1H, J = 1.2 Hz, $-H_{Naphthalene}$), 8.69 (d, 1H, J = 1.2 Hz, $-H_{Naphthalene}$), 8.25 (d, 2H, J = 2.6 Hz, $-H_{Carbazole}$), 7.95 (d, 1H, J = 7.8 Hz, $-H_{Naphthalene}$), 7.83 (dd, 2H, J_1 = 1.2 Hz, J_2 = 8.5 Hz, $-H_{Carbazole}$), 7.66 (t, 1H, $-H_{Naphthalene}$), 7.45–7.35 (m, 4H, $-H_{Carbazole}$), 4.31–4.15 (m, 2H, $-CH_2$, $-H_{aliphatic}$), 2.09–1.99 (m, 1H, –CH, $-H_{aliphatic}$), 1.56–1.24 (m, 8H, 4 × CH_2, $-H_{aliphatic}$), 1.09–0.82 (m, 6H, 2 × CH_3, $-H_{aliphatic}$). ^{13}C NMR spectrum (75.4 MHz, CDCl3, δ, ppm): 164.6, 164.2, 142.0, 140.4, 132.3, 131.9, 130.3, 129.2, 127.9, 127.6, 126.6, 124.0, 123.0, 120.9, 120.8, 110.2, 44.5, 38.2, 31.0, 28.9, 24.3, 23.4, 14.4, 10.9. IR, (in KBr), cm^{-1}: 3055 ν (CH_{ar}); 2958, 2923, 2878, 2856 ν ($CH_{aliphatic}$); 1699 ν ($C{=}O_{anhydride}$); 1634, 1652, 1587 ν ($C{=}C_{ar}$); 1457; 1333, 1235 ν (C–N); 782,789, 753, 746 γ (CH_{ar}). MS ($APCI^+$, 20 V), *m*/*z*: 490 ($[M+H]^+$). Anal. Calcd. for $C_{33}H_{34}N_2O_2$: C, 80.78; H, 6.98, N, 5.71; O, 6.52%; found C 80.86, H 6.76, N 5.84%.

2.3.8. (9-((N-(2-ethylhexyl)-1,8-naphthalimide)-4-yl)-3,6-di-tert-butyl-9H-carbazole (**12**)

(9-((*N*-(2-ethylhexyl)-1,8-naphthalimide)-4-yl)-3,6-di-*tert*-butyl-9*H*-carbazole (**12**) was prepared by the same procedure as **11** using 4-bromo-*N*-(2-ethylhexyl)-1,8-naphthalimide (**4**) (0.5 g, 1.29 mmol), 3,6-di-*tert*-butyl-9*H*-carbazole (1.52 g, 5.15 mmol). The crude product was purified by column chromatography using the mixture of ethyl acetate and hexane (1:9, *V*:*V*) as an eleuent to give almost pure **12**. Recrystallization from eluent gave pure **12** as yellow crystals. Yield: 71% (0.55 g), m.p. 133–134 °C; ^{1}H NMR spectrum (300 MHz, CDCl3, δ, ppm): 8.81 (d, 1H, J = 7.8 Hz, $-H_{Naphthalene}$), 8.72 (d, 1H, J = 1.2 Hz, $-H_{Naphthalene}$), 8.70 (d, 1H, J = 1.2 Hz, $-H_{Naphthalene}$), 8.26 (d, 2H, J = 1.9 Hz, $-H_{Carbazole}$), 7.90 (d, 1H, J = 7.8 Hz, $-H_{Naphthalene}$), 7.67 (t, 1H, $-H_{Naphthalene}$); 7.48 (dd, 2H, J_1 = 2.0 Hz, J_2 = 3.1 Hz, $-H_{Carbazole}$), 7.38–7.34 (m, 2H, $-H_{Carbazole}$), 4.31–4.19 (m, 2H, $-CH_2$, $-H_{aliphatic}$), 2.09–2.02 (m, 1H, –CH, $-H_{aliphatic}$), 1.52 (s, 18H, 6 × CH_3, $-H_{aliphatic}$), 1.49 (s, 8H, 4 × CH_2, $-H_{aliphatic}$), 1.05–0.95 (m, 6H, 2 × CH_3, $-H_{aliphatic}$). ^{13}C NMR spectrum (75.4 MHz, CDCl3, δ, ppm): 144.0, 142.4, 140.4, 138.2, 132.2, 131.9, 130.6, 129.1, 127.6, 127.1, 124.2, 123.7, 122.5, 116.7, 116.4, 110.2, 109.7, 44.5, 38.2, 35.0, 32.2, 31.0, 29.0, 24.3, 23.4, 14.4, 10.9. IR, (in KBr), cm^{-1}: 3053 ν (CH_{ar}); 2955, 2921, 2874, 2856 ν ($CH_{aliphatic}$); 1701, 1699 ν ($C{=}O_{anhydride}$); 1623, 1651, 1587 ν ($C{=}C_{ar}$); 1457; 1333, 1235 ν (C–N); 779,789, 751, 742 γ (CH_{ar}). MS ($APCI^+$, 20 V), *m*/*z*: 602

([M+H]$^+$). Anal. Calcd. for $C_{41}H_{50}N_2O_2$: C, 81.69; H, 8.36; N, 4.65; O, 5.31%; found C 81.45, H 8.28, N 4.43%.

2.3.9. *((E)-9-(((N-(2-ethylhexyl)-1,8-naphthalimide)-4-yl)ethenyl)-9H-carbazole (**13**)*

A round bottom flask was charged with a mixture of 4-bromo-*N*-(2-ethylhexyl)-1,8-naphthalimide (**4**) (0.5 g, 1.29 mmol), *N*-vinylcarbazole (0.40 g, 1.93 mmol), $Pd(OAc)_2$ (0.005 g, 0.016 mmol), P(*o*-tolyl)$_3$ (0.016 g, 0.071 mmol), DMF (8 mL) and triethylamine (2 mL). The flask was degassed and purged with N_2. The reaction mixture was heated at 90 °C for 24 h under nitrogen. Then, it was filtered and the filtrate was poured into methanol. The yellow precipitate was filtered, washed with methanol and dissolved in methylene chloride. After evaporation of the solvent, the crude product was purified by silica gel column chromatography using the mixture of ethylacetate and *n*-hexane (1:9, *V*:*V*) as an eluent and crystallized from the eluent mixture of solvents to give **13** as yellow crystals. Yield 32% (0.21 g), m.p. = 214–215 °C. ^{1}H NMR spectrum (300 MHz, CDCl3, *δ*, ppm):8.71 (d, 1H, *J* = 1.1 Hz, $-H_{Naphthalene}$), 8.69 (d, 1H, *J* = 1.1 Hz, $-H_{Naphthalene}$), 8.57 (d, 1H, *J* = 1.1 Hz, $-H_{Naphthalene}$), 8.55 (d, 1H, *J* = 1.1 Hz, $-H_{Naphthalene}$), 8.17 (d, 2H, *J* = 7.7 Hz, $-H_{Carbazole}$), 8.06 (d, 1H, *J* = 2.5 Hz, $-H_{Naphthalene}$), 7.90–7.83 (m, 4H, $-H_{Carbazole}$, -vinylic), 7.62–7.55 (m, 2H, $-H_{Carbazole}$), 7.46–7.39 (m, 2H, $-H_{Carbazole}$), 4.23–4.14 (m, 2H, $-CH_2$, $-H_{aliphatic}$), 1.91–1.86 (m, 1H, −CH, $-H_{aliphatic}$), 1.49–1.33 (m, 8H, 4 × CH_2, $-H_{aliphatic}$), 1.03–0.88 (m, 6H, 2 × CH_3, $-H_{aliphatic}$). ^{13}C NMR spectrum (75.4 MHz, CDCl3, *δ*, ppm): 164.6, 164.1, 141.7, 140.6, 139.8, 132.3, 131.9, 130.3, 129.4, 129.2, 127.9, 127.6, 126.6, 124.1, 123.0, 120.9, 120.4, 110.3, 45.5, 37.8, 32.1, 28.8, 25.4, 23.5, 14.3, 10.9. IR, (in KBr), cm^{-1}: 3052 ν (CH_{ar}); 2956, 2924, 2878, 2856 ν ($CH_{aliphatic}$); 1700 ν ($C{=}O_{anhydride}$); 1634, 1652, 1587 ν ($C{=}C_{ar}$); 1457; 1333, 1235 ν (C–N); 955 γ (trans, CH=CH); 782,789, 753, 746 γ (CH_{ar}). MS (APCI$^+$, 20 V), *m*/*z*: 500 ([M+H]$^+$). Anal. Calcd. for $C_{34}H_{32}N_2O_2$: C, 81.57; H, 6.44; N, 5.60; O, 6.39%; found C 81.76, H 6.58, N 5.48%.

3. Results and discussion

3.1. Synthesis and characterization

Compounds **5**–**13** were synthesized as shown in Scheme 1 by Suzuki-Miyaura coupling reactions of compound **4** with 1.1 equiv. of 9-alkyl-3-(4,4,5,5-tetramethyl[1,3,2]dioxaborolan-2-yl)-9*H*-carbazole or 2.2 equiv. of 9-alkyl-3,6-(4,4,5,5-tetramethyl[1,3,2] dioxaborolan-2-yl)-9*H*-carbazole catalyzed by $Pd(PPh_3)_4$.

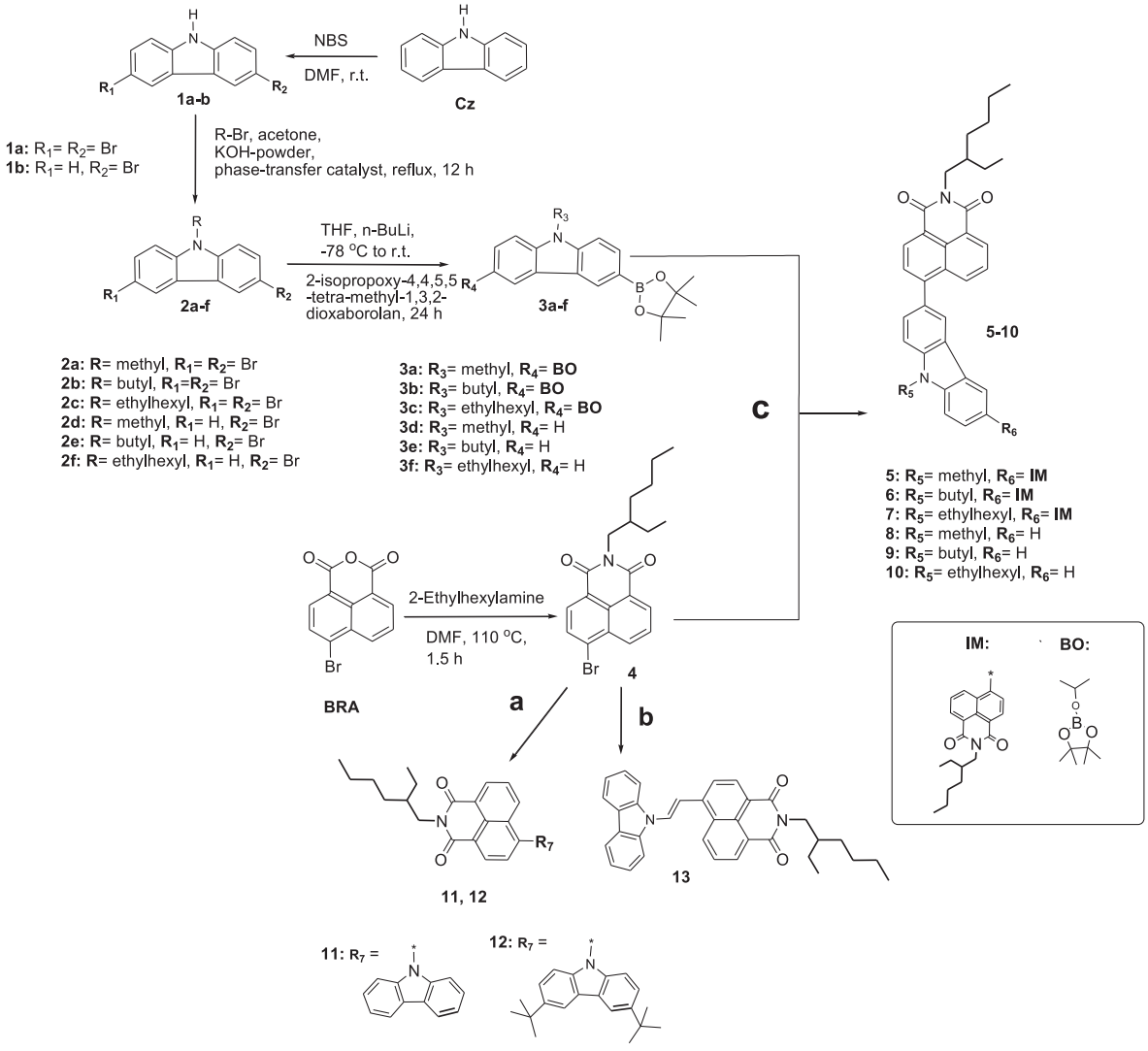

Scheme 1. The synthetic routes to compounds **5**–**13**. Reagents and conditions: (a) 9*H*-carbazole or 3,6-di(*tert*-butyl)-9*H*-carbazole, Cu, 18-crown-6, K_2CO_3, *o*-dichlorobenzene, 180 °C, 24 h; (b) *N*-vinylcarbazole, $Pd(OAc)_2$, P(*o*-tolyl)$_3$, DMF, TEA, 90 °C, 24 h; (c) aromatic boronic acid pinacol ester, $Pd(PPh_3)_2Cl_2$, THF/H_2O, K_2CO_3, 80 °C, 24 h.

Compounds **11** and **12** were synthesized by Ullmann type condensation of compound **4** with 9*H*-carbazole or 3,6-di(*tert*-butyl)carbazole, respectively. Compound **13** was obtained by Heck reaction of bromo derivative **4** with *N*-vinylcarbazole in the presence of palladium(II) acetate and tri-*o*-tolylphosphine. All the crude products were purified by silica gel column chromatography to obtain compounds **5**–**13** in the yields of 32–71%. All the target compounds were characterized by ^{1}HNMR, ^{13}C NMR, IR and elemental analysis. They exhibited good solubility in common organic solvents such as dichloromethane (DCM), chloroform, tetrahydrofuran (THF), chlorobenzene, dioxane, toluene.

3.2. Theoretical calculations

Quantum chemical calculations of the carbazole and naphthalimide derivatives were performed using density functional theory (DFT) as implemented in the Gaussian 09 [69] software package. Ground-state geometries of the molecular structures were optimized at the B3LYP functional level with the 6-31G(d) basis set supplemented with polarization functions. Singlet transition energies, the corresponding oscillator strengths, and spatial distributions of electron density for the highest occupied molecular orbital (HOMO) and the lowest unoccupied molecular orbital (LUMO) were obtained by means of the semi empirical ZINDO calculations. The DFT calculations revealed similar electronic energy spectra, and electron density distributions for the monosubstituted and bisubstituted compounds **5**–**12** up to the S_3 state. Higher-lying states will not be considered in the further discussion.

Fig. 1 shows optimized geometries and charge density distributions in the HOMO and LUMO states for compounds **5**, **8**, **11** and **13** (for more details on the calculated electron density distributions for HOMO and LUMO molecular orbitals of carbazole and 1,8-naphthalimide derivatives (**6, 7, 9, 10** and **12**) see in the Supplementary Information (SI)).

The compounds show significant variation in the rotation angle between the planes of naphthalimide and carbazole moieties (here 0° angle denote planar configuration). Compounds **5**–**10** in which carbazole is linked to 1,8-naphthalimide moiety at C-3 position show rotation angle of 51°, while compounds **11**, **12** in which carbazole is linked to 1,8-naphthalimide at N-9 position show larger angle of 60°, while compound **13** having ethenyl-containing linkage between N-9 position of carbazole and C-4 position of 1,8-naphthalimide shows almost flat configuration with rotation angle of only 14°. It is evident that the HOMO state comprises charge redistribution from the naphthalimide and carbazole moieties, where the impact of carbazole orbitals is governed by the rotation angle. Derivatives of carbazole having two 1,8-naphthalimide moieties (**5**–**7**) show broader electron density distribution extending on both naphthalimide moieties (compound **5**). The charge density in the LUMO state is predominantly localized on the naphthalimide moieties for all the compounds.

To obtain the information on the states of different conformers of the singly bridged multichromophoric compounds, the optimization was performed for various dihedral angles between the planes of neighboring carbazole and naphthalimide units. Fig. 2 shows calculated energies of the ground S_0 and excited S_1, S_2 and S_3 states and of the corresponding oscillator strengths of the transitions, for compounds **8** and **11**, in which carbazole moiety is linked to 1,8-naphthalimide species via its C-3 and N-9 positions, correspondingly.

The energies and oscillator strengths exhibited some angular asymmetry with respect to a 90° angle due to asymmetry introduced by orientation of the alkyl chains. The optimization of the total energies revealed flat energy minima of the ground S_0 and excited S_1, S_2 and S_3 states with respect to the dihedral angle between the naphthalimide and carbazole moieties. For the upward transitions from S_0, the maximum accessible dihedral angle is limited by the molecule energy, which is of the order of the thermal energy. The broad energy minimum of the D-A type derivatives of carbazole and naphthalimide extending over the angles of 40–130° implied molecules with a large variety of twist angles available in the ground state at room temperature. This also indicates weak steric effects between the fragments for the dihedral angles within this range. There is also interplay between the lowest S_1 S_2 and S_3 transitions that involve different molecular orbitals within allowed range of the twisting angles. For the C-3 linked compound **8** (Fig. 2(b)) the largest oscillator strength of 0.75 shows S_0–S_2 transition which is formed by of π-π molecular orbitals. Note, that the energy distance between the S_1 and S_2 states is small, >0.1 eV and for rotation angle of 43° this S_2 state becomes the lowest energy state. For N-9 linked compound **11** (Fig. 2(b)) the allowed S_2 state shows remarkably smaller oscillator strength of 0.33 for S_0–S_2 transition at the optimized twisting angle of 61°. The reduction of the oscillator strength of the lowest allowed transition is typical feature of N-9 linked carbazole moieties due to enhanced impact of n-π orbitals [40]. The lowest energy S_0–S_1 transition is of low oscillator strength of 0.004. The energy separation between S_1 and S_2 states is of 0.13 eV. Owing to the almost flat configuration compound **13**, having ethenyl-containing linkage between N-9 position of carbazole and C-4 position of 1,8-naphthalimide shows allowed S_0–S_1 transition with the oscillator strength of 0.95.

3.3. Thermal properties

The thermal transitions of compounds **5**–**13** were studied by DSC and TGA under a nitrogen atmosphere. The values of glass transition temperatures (T_g), melting points (T_m), crystallization temperatures (T_{cr}) and 5% weight loss temperatures ($T_{dec\text{-}5\%}$) are summarized in Table 1.

The synthesized derivatives exhibit high thermal stability. Their 5% weight loss temperatures exceed 351 °C. Compounds **5**–**13** were isolated after the synthesis as crystalline materials. Their first DSC heating scans revealed endothermal melting signals in the range of 108–224 °C. No crystallizations were observed during the cooling scans, which indicated direct transitions from the melt to glassy states. In the second DSC heating scans, the compounds exhibited glass transitions with glass transition temperatures ranging from 30 to 101 °C. Glass transition temperature of compounds **9** and **10** were found to be below the room temperature, therefore these compounds cannot be classified as molecular glasses. The DSC thermograms of compound **8** are given in Fig. 3.

The first DSC scan of compound **8** revealed melting at 127 °C, whereas after cooling the second heating scan revealed glass transition at 47 °C. Compounds **11** and **12** in which carbazolyl groups are directly linked via N-9 position to the 1,8-naphthalimide moiety form glasses with the glass transition temperatures of 40 and 48 °C, respectively. Compound **13** in which carbazolyl group is linked to 1,8-naphthalimide moiety via the bridge containing double C=C bond, exhibiting almost flat geometry did not form glass upon cooling from the melt. It only showed melting at 224 °C. Nevertheless, amorphous films of compound **13** can be obtained by processing from solution. Compounds **5**–**7** having two 1,8-naphthalimide moieties exhibited considerably higher T_g than monosubstituted derivatives **8**–**10** with the corresponding alkyl substituents, apparently, because of their larger molecular weights, which result in the stronger intermolecular interactions. Incorporation of methyl, butyl and ethylhexyl nonconjugated substituents at the carbazole N-9 position progressively lead to the remarkable decrease in the T_g values both for monosubstituted (**8**–**10**) and bisubstituted (**5**–**7**) carbazole derivatives. Apparently, the flexible

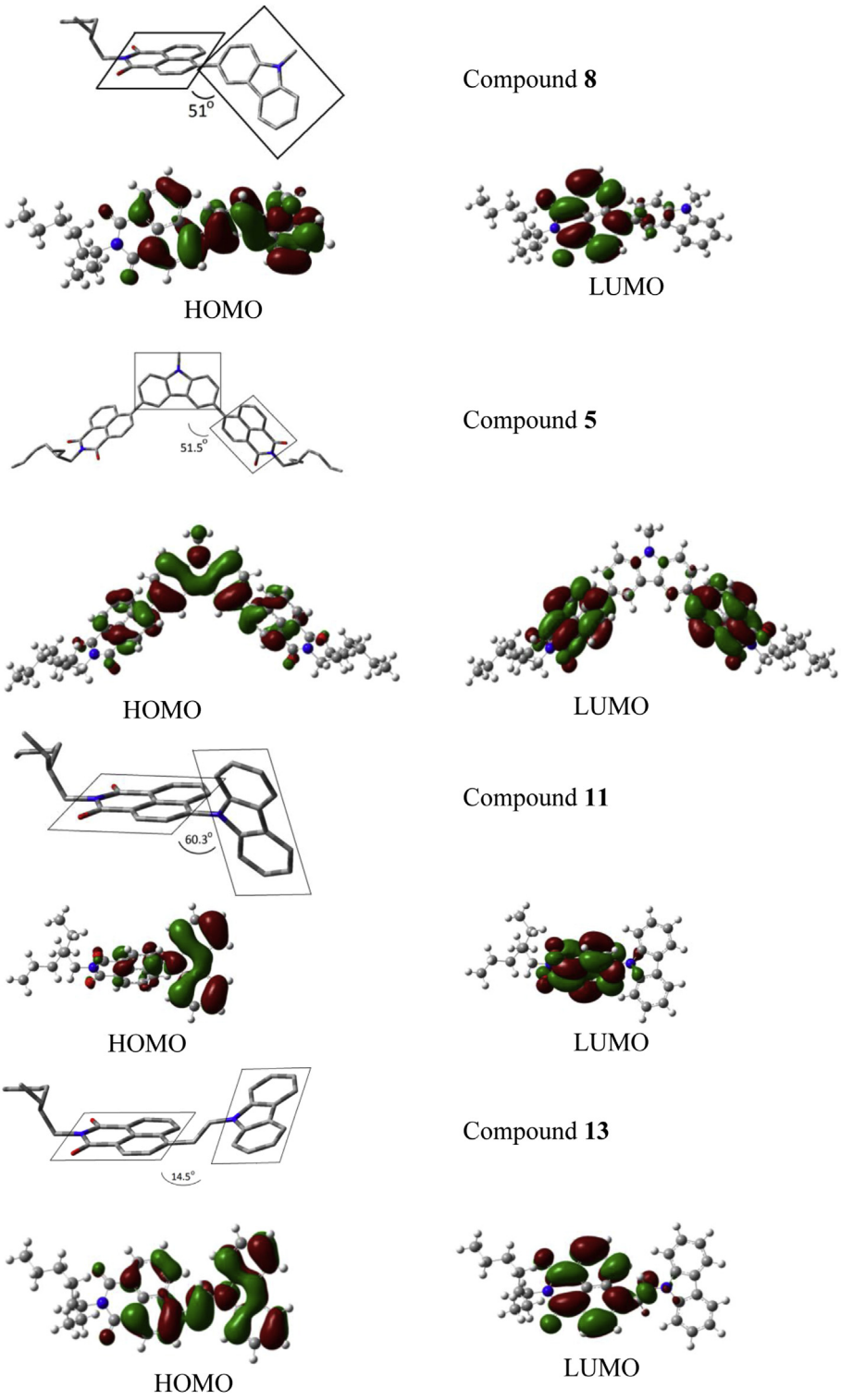

Fig. 1. Optimized geometries and calculated electron density distributions for HOMO and LUMO molecular orbitals of compounds **5**, **8**, **11** and **13**.

alkyl chains especially the branched ones, act as internal plasticizers of the molecular glasses preventing compact molecular packing.

3.4. Optical and photophysical properties

The absorption and normalized fluorescence spectra of the dilute solutions of compounds **5**–**13** in dilute THF, of the solid solutions in polystyrene matrix and the solid films of the pure compounds are shown in Figs. 4 and 5. The photophysical characteristics are summarized in Table 2.

First we will discuss optical properties of the compounds in which 1,8-naphthalimide moieties are linked at C-3 and C-6-positions of carbazolyl groups (compounds **5**–**10**). Dilute THF solutions of 3-monosubstituted and 3,6-disubstituted carbazole compounds exhibited two broad absorption bands at 344 nm and 398 nm

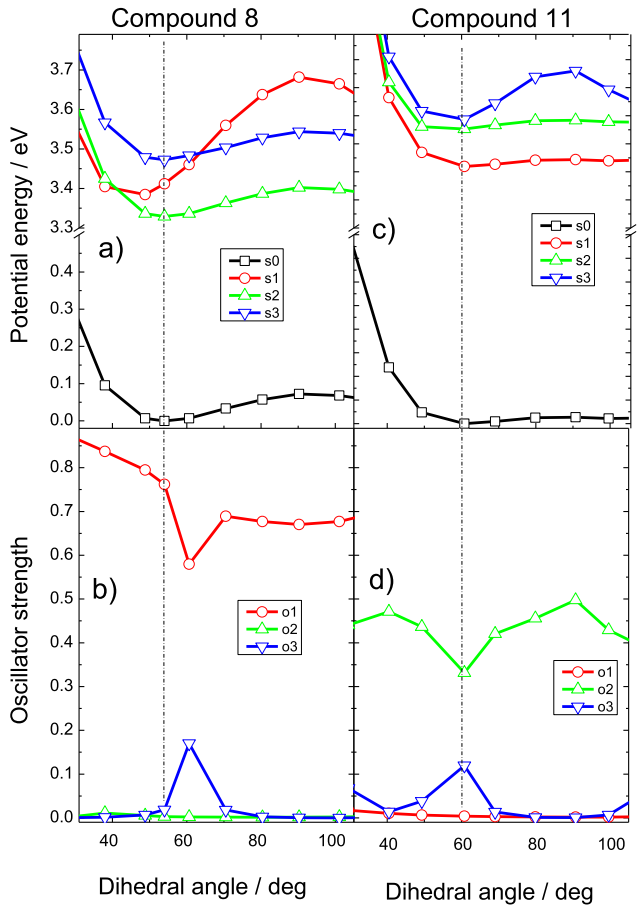

Fig. 2. Calculated energies of the ground S_0 and excited S_1, S_2 and S_3 states and of corresponding oscillator strengths of the transitions, for compounds **8** (a, b) and **11** (c, d).

which are typical for naphthalimide based donor-acceptor systems [29,70]. The absorption band at 344 nm can be attributed to the naphthalimide moiety [71], while the lowest energy absorption band can be attributed to the extended π-conjugated state involving the electron-donor carbazole and the electron-acceptor naphthalimide moieties. In accordance with the quantum chemical modeling, the values of oscillator strength of the lowest energy transitions of the bisubstituted carbazole compounds **5**–**7** are nearly twice as large as those of the monosubstituted counterparts **8**–**10** as a result of extended π-conjugation to the two naphthalimide moieties. Interestingly, increase of the length of alkyl

Table 1
Temperatures of the thermal transitions of compounds **5**–**13**.

Compound	T_g [°C](2nd heating)	T_m [°C]	T_{cr} [°C]	$T_{dec\text{-}5\%}$ [°C]
5	101	154	–	476
6	96	184	–	457
7	30	108	–	383
8	47	127	–	434
9	15	121	–	385
10	–5	110	–	351
11	40	117	–	373
12	48	140	–	417
13	–	224	176	422

Determined by DSC, scan rate 10 °C/min, N_2 atmosphere. T_m is melting point, T_g is glass transition temperature, T_{cr} is crystallization temperature. $T_{dec\text{-}5\%}$–5% weight loss temperatures; scan rate 20 °C/min, N_2 atmosphere.

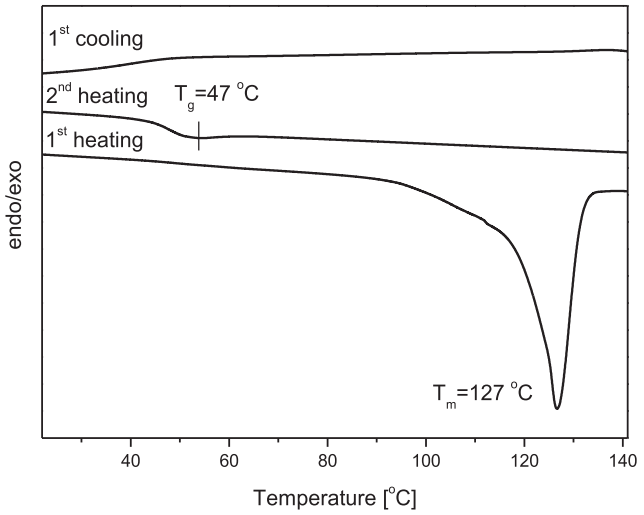

Fig. 3. DSC thermograms of compound **8** recorded at a heating/cooling rate of 10 °C min^{-1} under N_2.

substituents at the carbazole nitrogen atom results in the significant alteration of the intensity of the lowest energy absorption band in respect to the higher-energy naphthalimide absorption band. With the increase of the molecular weight of the alkyl substituent for monosubstituted compounds **8**–**10** the intensity of low-energy band decreases, while that of higher energy band increases. This observation can be attributed to the intramolecular twisting of the singly bonded donor-acceptor system. One can suggest that smaller substituents result in flatter geometry of the donor-acceptor system and thus, stronger absorbance of the lowest energy band.

Dilute solutions of mono- and disubstituted carbazole compounds **5**–**10** exhibited efficient fluorescence in the green spectral region with the bands peaking at 520–534 nm (Fig. 4). The Fluorescence spectra of the dilute solutions in polar THF are unstructured, broadened and strongly Stokes-shifted (by more than 120 nm). This observation indicates the pronounced intramolecular charge-transfer character of the excited states, which is typical for naphthalimide based donor-acceptor systems [72,73]. Generally, fluorescence spectra of compounds **5**–**10** exhibit similar fluorescence spectral properties which are in agreement with the results of DFT modeling showing delocalised orbitals in the HOMO state and almost similar localization of the excitation on the naphthalimide moiety in the LUMO state (see Fig. 4). The wavelengths of intensity maxima of fluorescence spectra of 3-monosubstituted carbazole derivatives are red-shifted by 10 nm in comparison with those of 3,6-disubstituted compounds. The significant red shift of ca. 60 nm of the fluorescence spectra of the dilute solutions in THF as compared to the spectra of the solid solutions in polystyrene matrix can be attributed to the polarity of the surrounding media. Pronounced positive solvatochromic effects are typical for naphthalimide based donor-acceptor systems [29,70]. Efficient fluorescence of the solid solutions of compounds **5**–**10** in nonpolar PS media correlate with the intensity of the lowest energy absorption band in accordance with variation of the radiative relaxation rate (see below). Relatively short radiative decay time of 6–8 ns observed for the compounds in which 1,8-naphthalimide moieties are linked at C-3 and C-6-positions of carbazolyl groups indicate on allowed transitions involving the lowest energy π–π orbitals, that can be further stabilized by the interaction with the solvent, what is in line with the results of DFT modeling.

Fluorescence quantum yields (η) of the compounds in polar THF solutions were determined to be in range of 0.66–0.83 for **5**–**10**,

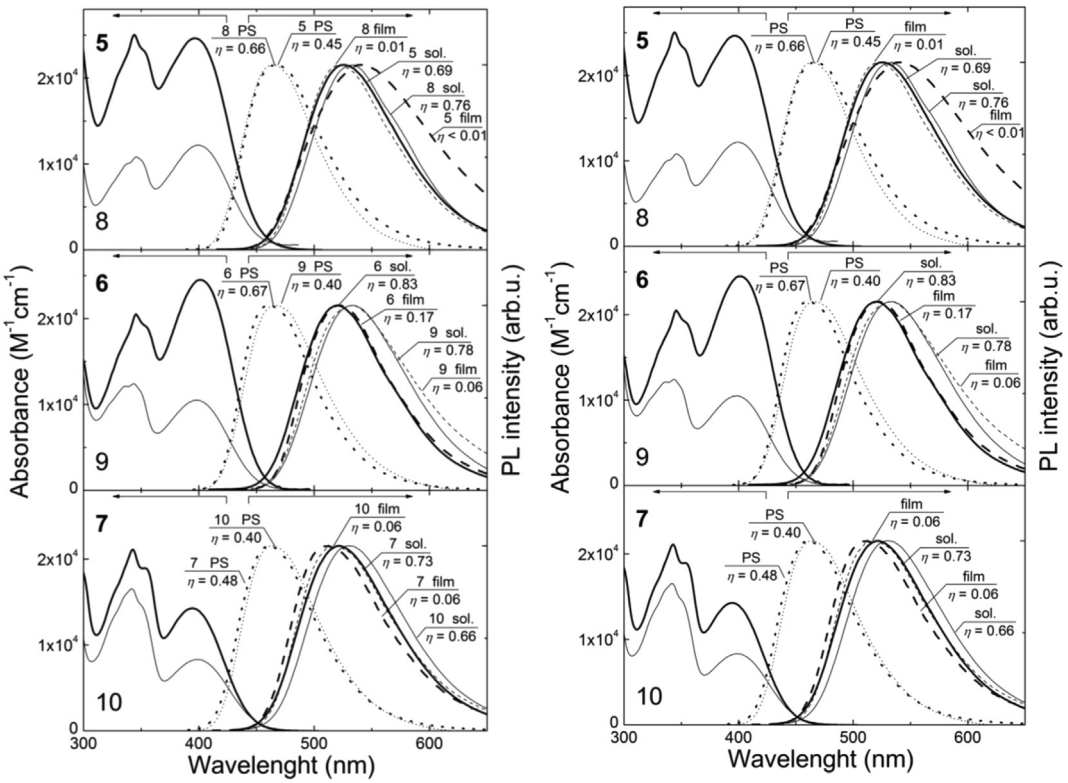

Fig. 4. Absorption and normalized fluorescence spectra of 1 μM solutions in THF (solid line), of the solid solutions in PS matrix at 1 wt% concentration (dotted line), and of the solid films (dashed line) of compounds **5**–**7** (thick line) and **8**–**10** (thin line). Fluorescence quantum yields (η) are indicated.

while for compounds **5**–**10** embedded in nonpolar PS matrices the values of η were found to be lower. They varied from 0.40 to 0.67. The enhancement of η in polar solvents was attributed to the reduction of the influence of nonradiative recombination processes involving intersystem crossing [70,73]. Fluorescence spectra of the solid films of compounds **5**–**10** are slightly broadened and the values of η of the films were found to be lower from 5 to 76 times due to exciton migration quenching.

Excited state relaxation for the dilute solutions of compounds **5**–**10** in THF was found to follow the single exponential decay profile with estimated fluorescence lifetimes from 5.2 ns to 5.9 ns. The estimated fluorescence decay times for mono-substituted carbazole compounds were longer by 0.5–0.6 ns than those observed for bi-substituted derivatives (see Fig S2, (SI)). The incorporation of the compounds into solid PS matrix usually leads to restriction of the intramolecular vibrations and thus to reduction of the rate of non-radiative relaxation [74,75]. However in the case of compounds **5**–**10** the non-radiative decay rate was estimated to be 2–3 times higher in THF liquid media compared to the values estimated for the solid PS matrix. At the same time, the radiative decay rates of the dilute THF solutions and of the solid solutions in PS of the compounds showed only slight differences. Thus the increase of η in THF solutions occurs mainly due to the reduction of the non-radiative relaxation rate induced by the polarity of the surrounding media. The similar results were observed for naphthalimide systems possessing fluorene substituents and were attributed to the reduction of the intersystem crossing rate [70].

The alteration of the recombination rate constants, induced the increase of alkyl substituents at the nitrogen atom carbazole moiety, correlates well with the intensity of lowest energy absorption bands. For instance, the increase in molecular weight of compounds **8**–**10** results in the continuous increase of the radiative decay constant from 6.4 to 12 ns and synchronous decrease in the non-radiative decay constant from 12.3 to 8 ns of their solid solutions in PS. This observation can be attributed to the twisted conformation of the molecules in the ground state. Flatter molecular geometry results in stronger radiative transitions and lower rate of the non-radiative relaxation.

The decay transients of the solid films of compounds **5**–**10** exhibited non-exponential behavior with average decay times shorter than those observed for the dilute solutions. Since the decay curves of the solid solutions in PS are single exponential, one can attribute the shortening of the lifetimes in the wet casted solid films to the dispersive exciton hopping [76].

The absorption and normalized fluorescence spectra of dilute THF solutions, solid solutions in polystyrene matrix and of solid films of the investigated carbazole and 1,8-naphthalimide derivatives **11**–**13** are shown in Fig. 5. The photophysical characteristics of compounds **11**–**13** are summarized in Table 2. Generally the absorption spectra of the compounds (**11**–**13**) in which carbazolyl groups are linked via N-9 position to the 1,8-naphthalimide moiety show two similar bands as the absorption spectra of 1,8-naphthalimide derivatives with the carbazolyl groups linked at C-3 and C-6 carbazole positions, however the lowest energy absorption band of the former compounds is significantly red-shifted (up to 38 nm). The red shift can be attributed to the low lying n–π states of carbazole moiety [40]. The optical properties of compounds **11** and **12** significantly differ from those of compound **13**. As revealed by DFT modeling, the singly bonded compounds **11** and **12** exhibit significantly twisted molecular geometry, while compound **13** with ethenyl-containing linkage between the chromophores possesses almost flat geometry. This is in line with almost 6-fold enhancement of the low-energy band oscillator strength of

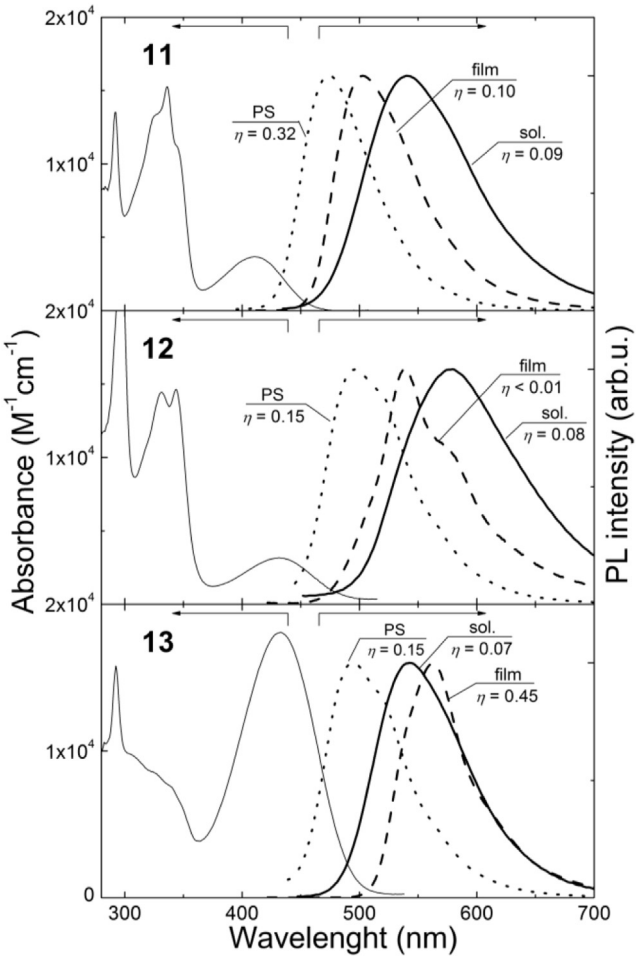

Fig. 5. Absorption and normalized fluorescence spectra of 1 μM solution in THF (solid line), of the solid solutions in PS matrix at 1 wt% concentration (dotted line), and of the solid films (dashed line) of compounds **11**–**13**. Fluorescence quantum yields (η) are indicated.

compound **13** with respect respect to those of compounds **11** and **12** (see Fig. 1).

Dilute solutions of compounds **11**–**13** exhibited broad unstructured fluorescence bands peaking at 540–579 nm. The estimated fluorescence quantum yields of the solutions were in the range of 0.07–0.09. These values were found to be more than 10-fold lower than those estimated for the derivatives **5**–**10** in which 1,8-naphthalimide moieties are linked at C-3 or C-3,6-positions of carbazole ring. Fluorescence decay times for compounds **11** and **12** were 7 and 7.7 ns respectively, while compound **13**, possessing ethenyl-containing linkage, demonstrated 10-fold faster fluorescence decay. In accordance with the variation of the oscillator strength of the lowest energy absorption band, the radiative decay time of compounds **11** and **12** is 5–6 times larger than that of compound **13**. This is in line with the results of DFT modeling, indicating on forbidden S_1–S_0 transition for strongly twisted compound **11** in contrast to compound **13** possessing almost flat geometry. Interestingly, the rate of non-radiative recombination is also significantly faster for compound **13**. In case of the linkage via N-9 position of carbazole moiety the impact of polarity of the surrounding media has opposite effect as compared to C-3 linked compounds. The rate of non-radiative relaxation is decreasing by a factor of 2–3 in a nonpolar media. We attribute this observation to the peculiarities of the intersystem crossing rate of the compounds in which carbazolyl group is linked via N-9 position.

The solid films of the carbazole derivatives substituted at N-9 position demonstrated fluorescence spectra with the band peaks at 501, 537 and 563 nm for compounds **11**, **12** and **13**, respectively. Fluorescence spectra of the solid films of compounds **11** and **12** were found to be significantly blue shifted in comparison with the spectra of THF solutions. Solid state spectra exhibit well expressed vibronic structures indicating the regular packing of the molecules. It should be stressed that compound **13**, possessing almost flat geometry, exhibited very efficient fluorescence in the solid state with η as high as 0.45, which is significantly higher than that of isolated molecules in liquid solution in THF and in solid solution in PS. The significant red shift and narrowing of the fluorescence spectrum indicate the ordered packing and enhanced excitonic interaction in the film of compound **13**. The enhancement of the average fluorescence lifetime in the film and the increase of η indicate significant reduction of the non-radiative relaxation rate. The similar tendency was observed for anthracene crystals, where the significant reduction of the intersystem crossing rate was attributed to the increased exciton coupling in the crystal [77,78].

3.5. Electrochemical and photoelectrical properties

The electrochemical properties of compounds **5**–**13** were examined by cyclic voltammetry (CV). The measurements were carried out at 25 °C in CH_2Cl_2 solution containing 0.1 M tetrabutylammonium hexafluorophosphate (Bu_4NPF_6) as supporting

Table 2
Photophysical properties of the dilute THF solutions, solid films and 1 wt% solid solutions in PS matrixes of compounds **5**–**13**.

Compound	Liquid solution in THF						Neat film			Solid solution in PS				
	λ_{abs}(nm)[a] (ε[b], L mol^{-1} cm^{-1})	λ_F^{max} (nm)[c]	η	τ (ns)	τ_R (ns)[d]	τ_{NR} (ns)[d]	λ_F^{max} (nm)[c]	η	τ (ns)	λ_F^{max} (nm)[c]	η	τ (ns)	τ_R (ns)[d]	τ_{NR} (ns)[d]
5	344 (25,061) 397 (24,643)	522	0.69	5.4	7.8	17.4	541	<0.01	0.2 [57%], 1.1 [30%], 6.4 [13%]	468	0.45	3.8	8.4	6.9
6	345 (24,256) 398 (25,014)	520	0.83	5.2	6.3	30.6	522	0.17	4.4 [52%], 1.2 [27%], 17.7 [21%]	461	0.67	4	5.9	12.1
7	343 (21,113) 395 (14,277)	522	0.73	5.2	7.1	19.3	513	0.06	1.8 [56%], 0.4 [28%], 5.9 [16%]	461	0.48	3.7	7.7	7.1
8	345 (10,833) 398 (12,202)	533	0.76	5.9	7.8	24.6	522	0.01	0.3 [46%], 1.1 [39%], 4.3 [15%]	465	0.66	4.2	6.4	12.3
9	344 (12,413) 398 (10,505)	534	0.78	5.8	7.4	26.4	533	0.07	2.3 [47%], 0.5 [34%], 11.4 [19%]	466	0.55	4.1	7.5	9.1
10	342 (16,553) 398 (8296)	529	0.66	5.7	8.6	16.8	519	0.06	1.0 [62%], 0.3 [31%], 3.5 [7%]	462	0.40	4.8	12	8
11	336 (15,253) 413 (3660)	540	0.09	7	58.3	7.9	501	0.10	4.9 [49%], 9.8 [45%], 1.1 [6%]	474	0.32	13.8	43.1	20.3
12	344 (14,647) 432 (3167)	579	0.08	7.7	51.3	9.1	537	<0.01	0.3 [47%], 1.0 [43%], 3.3 [10%]	496	0.15	13.8	92	16.2
13	433 (18,078)	542	0.07	0.7	10	0.8	563	0.45	4.5 [83%], 1.9 [17%]	495	0.15	2.6	17.3	3.1

[a] Peak wavelength of absorption bands.
[b] Molar extinction coefficient.
[c] Wavelength of fluorescence band maximum.
[d] Radiative and non-radiative decay time constants calculated as τ/η and $\tau/(1-\eta)$, respectively.

electrolyte with a glassy carbon working electrode. The oxidation potentials were measured vs $Ag/AgNO_3$ as the reference electrode. Taking 4.8 eV as the ionization potential (IP_{CV}) value for the ferrocene redox system related to the vacuum level, the IP_{CV} and electron affinity (EA_{CV}) values of compounds **5**–**13** were calculated. The results of the CV measurements are shown in Table 3.

Compounds **5**–**13** exhibited irreversible oxidation/reduction processes, which could be assigned to one-electron oxidation of carbazole moiety at positive potential range (localized at 0.66–0.96 V) and quasi-reversible reduction/reoxidation processes at negative potential range (localized at −1.76 to −1.88 V). 3,6-Disubstituted carbazoles **5**–**7** showed much higher oxidation potentials (0.88 V (for **5**), 0.87 V (for **6**) and 0.95 V (for **7**)) compared to 3-substituted carbazoles **8**–**10** (0.77 V (for **8**), 0.77 V (for **9**) and 0.78 V (for **10**)) (Table 3). The similar positions of cathodic reduction peaks indicate that naphthalimide moieties are responsible for these processes. The solid state ionization potentials established by CV (IP_{CV}) range from 5.45 to 5.76 eV. In the 3-substituted carbazoles **8**–**10** the donoric fragment apparently has stronger influence on the electrochemical properties as compared to 3,6-disubstituted carbazoles **5**–**7**. For this reason, 3-substituted carbazoles **8**–**10** show lower IP_{CV} values as compared to those of 3,6-disubstituted carbazoles **5**–**7**.

Since C-3- and C-6-positions of carbazole moieties in compounds **5**–**7** are occupied, repeated 5 oxidation cycles of the solutions of these compounds do not show any changes in the CV curves. This is an evidence of the electrochemical stability of the 3,6-disubstituted carbazoles (**5**–**7**). Meanwhile the electron-rich and highly activated 6-positions of 3-substituted carbazoles **8**–**10** are very sensitive towards electrochemical oxidation, which may lead to dimerization reactions [79] and dimer formation in the potential range 0–1 V, and hence to a lower electrochemical stability (Fig. 6(a–c)).

Among 9-substituted carbazoles **11**–**13** the oxidation potentials are in the order: **11** > **12** > **13**. The EA_{CV} levels of compounds **5**–**13**, which are related to the onset reduction potentials, are close to each other (Table 3).

9-Substituted carbazole derivative **11** has active 3,6-positions of the carbazole moiety and therefore undergoes electrochemical polymerization and the film formation on the electrode surface (Fig. 6(e)). The polymeric film formation is evidenced by the successive growth of the current within the potential range −2 to 1.3 V.

Table 3
Electrochemical characteristics of **5**–**13**.

Compound	E^{ox}_{onset} vs Fc/V[a]	E^{red}_{onset} vs Fc/V[a]	IP_{CV} [eV][b]	EA_{CV} [eV][b]	E^{elc}_{g}[eV][c]	E^{opt}_{g} [eV][d]	IP_{EP}, [eV][e]
5	0.88	−1.87	5.68	−2.94	2.75	2.57	5.95
6	0.87	−1.85	5.67	−2.95	2.72	2.55	5.98
7	0.95	−1.86	5.75	−2.94	2.81	2.78	6.00
8	0.77	−1.87	5.56	−2.94	2.61	2.40	5.78
9	0.77	−1.88	5.55	−2.93	2.63	2.75	5.76
10	0.78	−1.88	5.58	−2.92	2.66	2.58	5.93
11	0.96	−1.76	5.76	−3.04	2.72	2.73	6.09
12	0.66, 0.86	−1.79	5.46	−3.01	2.45	2.50	5.81
13	0.66	−1.80	5.45	−3.00	2.46	2.51	5.69

[a] E^{ox}_{onset} and E^{red}_{onset} are measured vs. ferrocene/ferrocenium.
[b] Ionization potentials and electron affinities estimated according to $IP_{CV} = (E^{ox}_{onset} + 4.8)$ [eV]. $EA_{CV} = -(E^{red}_{onset} + 4.8)$ [eV] (where, E^{ox}_{onset} and E^{red}_{onset} are the onset reduction and oxidation potentials versus the Fc/Fc^{+}).
[c] $E^{elc}_{g} = |IP_{CV}| - |EA_{CV}|$, where E^{elc}_{g} is the electrochemical band gap.
[d] The optical band gap estimated from the onset wavelength of optical absorption according to the empirical formula: $E_g = 1240/\lambda_{edge}$, in which the λ_{edge} is the onset value of absorption spectrum in long wave direction.
[e] Established from electron photoemission in air spectra.

Compound **13** also has active 3,6-positions of the carbazole moiety and the repeated CV scans resulted in electrochemical polymerization of the compound (Fig. 6(e)). The CV curve of compound **12** shows two quasi-reversible oxidation peaks in the positive potential range (Fig. 6(f)). The first peak with the onset potential of 0.66 V can be ascribed to the oxidation of the electron-rich nitrogen atom in the carbazole core. The second peak, with the onset potential of 0.88 V can be attributed to oxidation of *tert*-butyl groups, which causes radical recombination and formation of a quinoid structure [80]. Repeated oxidation cycles did not change the redox potential what is an evidence of the electrochemical stability of the compound.

The ionization potential values, the layers of the synthesized compounds were also established by electron photoemission technique in air. Electron photoemission spectra of the amorphous films of compounds **5**–**13** are shown in Fig. 7. The values of the ionization potentials (IP_{EP}) are presented in Table 4.

The IP_{EP} values of amorphous layers of the synthesized compounds range from 5.57 to 6.01 eV. The values of solid state ionization potentials established by electron photoemission technique are by ca. 0.2–0.3 eV higher than those estimated by CV. However the trend of the IP_{EP} values is in agreement with that of IP_{CV}. 3,6-Disubstituted compounds **5**–**7** and 9-substituted derivatives **11**, **12** exhibit a little higher ionization potentials than 3-monosubstituted compounds **8**–**10** and 9-substituted compound **13**.

Charge-transporting properties of carbazole and 1,8-naphthalimide derivatives were studied by CELIV technique at room temperature in air. The samples for CELIV measurements were prepared in the diode configuration by spin coating. Before the CELIV measurements using integral mode TOF technique we defined the holes as majority charge carriers of the studied carbazole and 1,8-naphthalimide derivatives. Fig. 8 shows photo-CELIV current transients of the amorphous layer of **5** for the different maximum voltage of the triangle pulse.

The capacitive charging current was found to be much higher than the current related to the conductivity of the derivative. The charge carrier mobilities were estimated by the formula $\mu = Kd^2/At^2_{max}$, where $K = 2/3$ for volume photogeneration charge carrier, d is the sample thickness, $A = U(t)/t$ is the voltage rise rate, t_{max} is extraction time when the maximum in the current transients is observed. The maximum was not clearly observed for the layer of **5** (Fig. 8) therefore for the estimation of t_{max} we subtracted the curves of the dark-CELIV current transients from the curves of the photo-CELIV current transients (Fig. 8, insert). The extraction time values (t_{max}) for the amorphous layer of compound **5** decreased from $2.2 \cdot 10^{-5}$ to $1.45 \cdot 10^{-5}$ s with the increase of the maximum voltage of the pulse from 10 to 20 V. This observation shows the increase of the mobility of charge carriers with the increase of the electric field. The CELIV current transients of the amorphous layers of other studied derivatives were similar to those of compound **5**. It was not possible to measure charge motilities for derivatives **9** and **10** since their glass transition temperatures are lower than the room temperature and it was difficult to get a top Al electrode on the layers of these derivatives.

The hole mobility data for compounds **5**–**7** and **11**–**13** established by CELIV are summarized in Table 4. All the studied derivatives of carbazole and 1,8-naphthalimide display the hole mobility values of the order of 10^{-6} $cm^2/V \cdot s$ at the electric fields of the range of $(3.6–8.1) \cdot 10^5$ V/cm, with only a minor effect of the substitution pattern and the linking topology on the hole mobilities. These mobility values are lower compared to those of donor–acceptor molecules consisting of triphenylamine core and 1,8-naphthalimide arms [81], and of naphthalimide-substituted fluorene derivatives [70]. The charge mobilities of the earlier

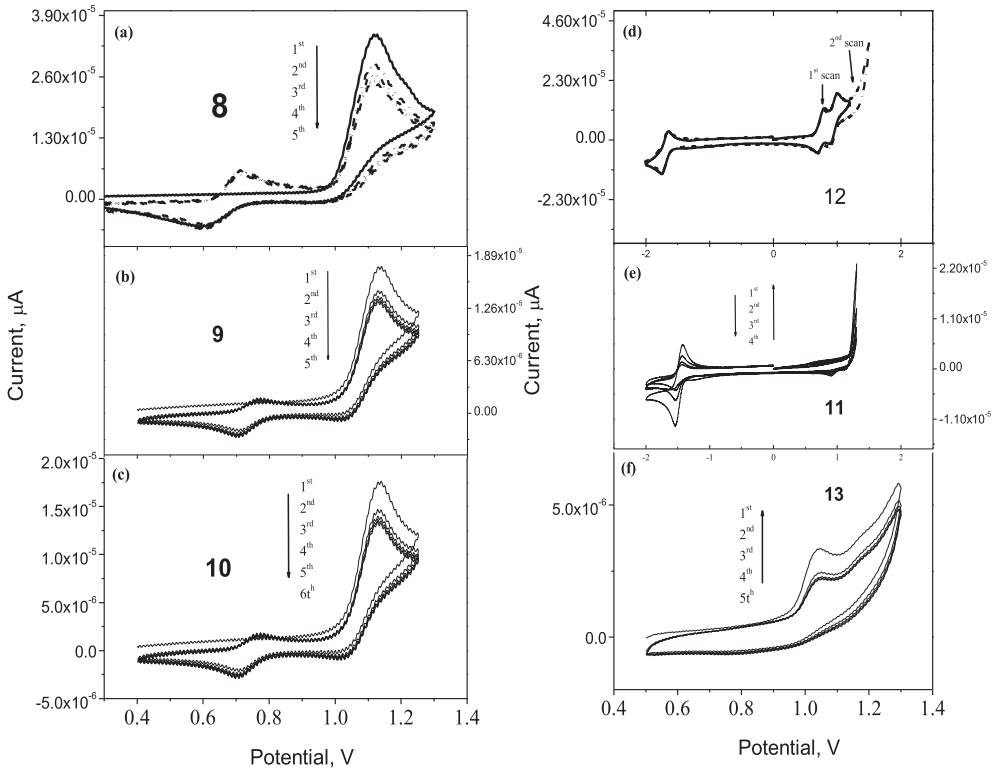

Fig. 6. Cyclic voltammograms of compounds **5**–**13** (10^{-5} M solutions, scan rate of 50 mV s^{-1} vs Ag/Ag^{+}) in 0.1 M solution of Bu_4NPF_6 in CH_2Cl_2.

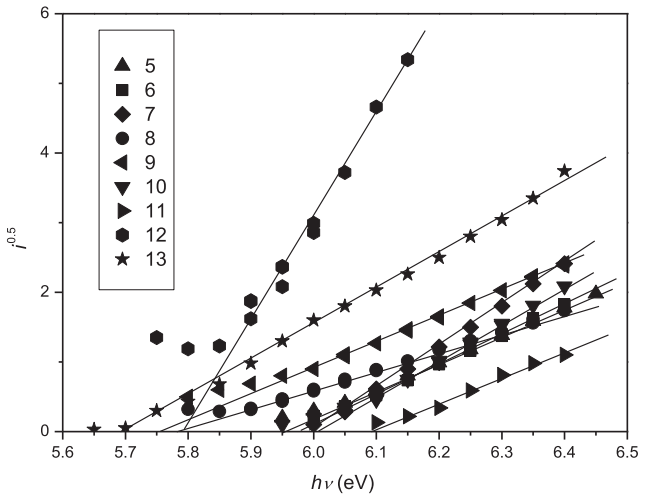

Fig. 7. Electron photoemission spectra of the layers of compounds **5**–**13**.

reported derivatives were estimated by xerographic time of flight (XTOF) technique. The charge mobility values of the films of compounds **5**–**8**, **11**–**13** could be higher if measured it by time of flight (TOF) [82] or by organic field effect transistor (OFET) technique [83].

4. Conclusions

A series of 1,8-naphthalimide and carbazole derivatives with different substitution patterns and different linking topologies were synthesized via palladium-catalyzed reactions. These compounds exhibit high thermal stability with 5% weight loss temperature up to 476 °C. Most of the synthesized compounds are capable of glass formation with glass transition temperatures from 30 to 87 °C. Optical properties of the singly bonded carbazole electron-donor and naphthalimide electron-acceptor systems were rationalized in the frames of the model of intramolecular charge-transfer states, which is confirmed by DFT modeling and analysis of the excited state properties in the media of various polarity and viscosity. Naphthalimide and carbazole donor-acceptor systems show broad unstructured fluorescence spectra peaking at 460–580 nm. Singly bonded 3-C-monosubstituted and 3,6-C-disubstituted compounds show pronounced positive solvatochromic effects with the reduction of the non-radiative recombination rate in polar solvents which results in high photoluminescence quantum yields up to 0.83. Increase of the length of alkyl substituents at N-9 position carbazole ring induces twisted conformation of the singly bonded naphthalimide and C-3-carbazole system. Strong intermolecular coupling of the flat derivative of 1,8-naphthalimide and carbazole possessing ethenyl-containing linkage in the solid state results in the significant enhancement of fluorescence quantum yield (up to 0.45) due to

Table 4
The charge carrier mobility data for the layers of the derivatives of carbazole and 1,8-naphthalimide established from CELIV transients at 20 V.

Compound	5	6	7	8	11	12	13
Thickness (d), nm	150	100	110	240	100	160	75
Mobility (μ), cm^2/V s	$1.43\cdot10^{-6}$	$2.37\cdot10^{-6}$	$0.87\cdot10^{-6}$	$1.6\cdot10^{-6}$	$3\cdot10^{-6}$	$0.47\cdot10^{-6}$	$0.14\cdot10^{-6}$

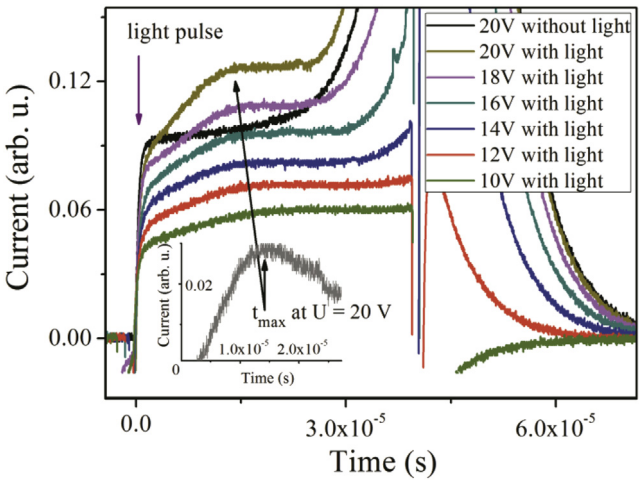

Fig. 8. The photocurrent extraction transients from the CELIV experiment for the layer of **5**.

supressed intersystem crossing rate. The ionization potentials of the synthesized compounds established by electron photoemisssion technique in air range from 5.46 eV to 5.76 eV. All the studied derivatives of carbazole and 1,8-naphthalimide display hole mobility values of the order of 10^{-6} $cm^2/V \cdot s$ at the electric fields in the range from $(3.6–8.1) \cdot 10^5$ V/cm.

Acknowledgments

This research was funded by the **European Social Fund** under the **Global Grant** measure. Habil. Dr. V. Gaidelis from the Department of Solid State electronics, Vilnius University is thanked for the help in the measurements of ionization potentials.

Appendix A. Supplementary data

Supplementary data related to this article can be found at http://dx.doi.org/10.1016/j.dyepig.2014.11.013.

References

[1] Yang JB, Ganesan P, Teuscher J, Moehl T, Kim YJ, Yi CY, et al. Influence of the donor size in d-pi-a organic dyes for dye-sensitized solar cells. J Am Chem Soc 2014;136:5722–30.
[2] Pron A, Reghu RR, Rybakiewicz R, Cybulski H, Djurado D, Grazulevicius JV, et al. Triarylamine substituted arylene bisimides as solution processable organic semiconductors for field effect transistors. Effect of substituent position on their spectroscopic, electrochemical, structural, and electrical transport properties. J Phys Chem C 2011;115:15008–17.
[3] Qu SY, Tian H. Diketopyrrolopyrrole (DPP)-Based materials for organic photovoltaics. Chem Commun 2012;48:3039–51.
[4] Reghu RR, Bisoyi HK, Grazulevicius JV, Anjukandi P, Gaidelis V, Jankauskas V. Air stable electron-transporting and Ambipolar Bay substituted perylene bisimides. J Mater Chem 2011;21:7811–9.
[5] Hunger K. Industrial dyes: chemistry, properties, application. Wiley-VCH; 2003.
[6] Gregory P. High technology applications of organic colorants. New York: Plenum; 1991. 15–5.
[7] Hrdlovic P, Chmela S, Danko M, Sarakha M, Guyot G. Spectral properties of probes containing benzothioxanthene chromophore linked with hindered amine in solution and in polymer matrices. J Fluoresc 2008;18:393–402.
[8] Samanta A, Ramachandram B, Saroja G. An investigation of the triplet state properties of 1,8-naphthalimide: a laser flash photolysis study. J Photochem Photobiol A 1996;101:29–32.
[9] Ye G, Zhao T, Jin Z, Gu P, Mao J, Xu Q, et al. The synthesis and NLO properties of 1,8-naphthalimide derivatives for both femtosecond and nanosecond laser pulses. Dyes Pigm 2012;94:271–7.
[10] Yin H, Zhu W, Xu Y, Dai M, Qian X, Li Y, et al. Novel aliphatic *N*-oxide of naphthalimides as fluorescent markers for hypoxic cells in solid tumor. Eur J Med Chem 2011;46:3030–7.
[11] Lai CM, Garner DM, Gray JE, Brogdon BL, Peterman VC, Pieniaszek HJ. Determination of bisnafide, a novel bis-naphthalimide anticancer agent, in human plasma by high-performance liquid-chromatography with UV detection. Pharm Biomed 1998;17:427–34.
[12] Zhang Y, Zhou C. Synthesis and activities of naphthalimide azoles as a new type of antibacterial and antifungal agents. Bioorg Med Chem Lett 2011;21:4349–52.
[13] Abad S, Kluciar M, Miranda MA, Pischel U. Proton-induced fluorescence switching in novel naphthalimide–dansylamide dyads. J Org Chem 2005;70:10565–8.
[14] Pina-Luis G, Martínez-Quiroz M, Ochoa-Terán A, Santacruz-Ortega H, Mendez-Valenzuela E. New dual emission fluorescent sensor for pH and Pb(II) based on bis(napthalimide) derivative. J Lumin 2013;134:729–38.
[15] Lv H, Liu J, Zhao J, Zhao B, Miao J. Highly selective and sensitive pH-responsive fluorescent probe in living hela and HUVEC cells. Sens Actuat B Chem 2013;177:956–63.
[16] Leng B, Tian HA. Unimolecular half-subtractor based on effective photoinduced electron transfer and intramolecular charge transfer processes of 1,8-naphthalimide derivative. Aust J Chem 2010;63:169–72.
[17] Lee J, Hsu SL. Green polymer-light-emitting-diodes based on polyfluorenes containing n-aryl-1,8-naphthalimide and 1,8-naphthoilene-arylimidazole derivatives as color tuner. Polymer 2009;50:5668–74.
[18] Yin S, Liu X, Li C, Huang W, Li W, He B. Electroluminescent properties of naphthalimide derivative thin film devices. Thin Solid Films 1998;325:268–70.
[19] Zhou, Chen P, Wang X, Wang Y, Wang Y, Li F, et al. Charge-transfer-featured materials-promising hosts for fabrication of efficient OLEDs through triplet harvesting *via* triplet fusion. Chem Commun 2014;50:7586–9.
[20] Grabchev I, Moneva I, Bojinov V, Guittonneau S. Synthesis and properties of fluorescent 1,8-naphthalimide dyes for application in liquid crystal displays. J Mater Chem 2000;10:1291–6.
[21] Wanichacheva N, Prapawattanapol N, Lee VS, Grudpan K, Petsom A. Hg^{2+}-Induced self-assembly of a naphthalimide derivative by selective 'Turn-On' monomer/excimer emissions. J Lumin 2013;134:686–90.
[22] Kumar A, Vanita V, Walia A, Kumar SN. N,N-dimethylaminoethylaminoanthrone – a chromofluorogenic chemosensor for estimation of Cu^{2+} aqueous medium and HeLa cells imaging. Sens Actuat B Chem 2013;177:904–12.
[23] Qu Y, Hua J, Jiang Y, Tian H. Novel side-chain naphthalimide polyphenylacetylene as a ratiometric fluorescent chemosensor for fluoride ion. J Polym Sci Polym Chem 2009;47:1544–52.
[24] Cacialli F, Friend RH, Bouche CM, Barny LP, Facoetti H, Soyer F, et al. Naphthalimide side-chain polymers for organic light-emitting diodes: band-offset engineering and role of polymer thickness. J Appl Phys 1998;83:2343–56.
[25] Takahashi S, Nozaki K, Kozaki M, Suzuki S, Keyaki K, Ichimura A, et al. Photoinduced electron transfer of *N*-[(3- and 4-diarylamino)phenyl]-1,8-naphthalimide dyads: orbital-orthogonal approach in a short-linked d-a system. J Phys Chem A 2008;112:2533–42.
[26] Islam A, Cheng CC, Chi SH, Lee SJ, Hela GP, Chen IC, et al. Aminonaphthalic anhydrides as red-emitting materials: electroluminescence, crystal structure, and photophysical properties. J Phys Chem B 2005;109:5509–17.
[27] Yang JX, Wang XL, Wang XM, Xu LH. The synthesis and spectral properties of novel 4-phenylacetylene-1,8-naphthalimide derivatives. Dyes Pigm 2005;66:83–7.
[28] Magalhaes JL, Pereira RV, Triboni ER, Filho Berci P, Gehlen MH, Nart FC. Solvent effect on the photophysical properties of 4-phenoxy-*N*-methyl-1,8-naphthalimide. J Photochem Photobiol A 2006;183:165–70.
[29] Gudeika D, Grazulevicius JV, Sini G, Bucinskas A, Jankauskas V, Miasojedovas A, et al. New derivatives of triphenylamine and naphthalimide as ambipolar organic semiconductors: experimental and theoretical approach. Dyes Pigm 2014;106:58–70.
[30] Ding J, Gao J, Cheng Y, Xie Z, Wang L, Ma D, et al. Highly efficient green-emitting phosphorescent iridium dendrimers based on carbazole dendrons. Adv Funct Mater 2006;16:575–81.
[31] Palayangoda SS, Cao X, Adhikari RM, Neckers DC. Carbazole-based donor-acceptor compounds: highly fluorescent organic nanoparticles. Org Lett 2008;10:282–4.
[32] Yoonb KR, Byuna NM, Lee HS. Synthesis and characterization of carbazole-based nonlinear optical polymers possessing chromophores in the main or side chains. Synth Met 2007;157:603–10.
[33] Liu C, Li Y, Zhang Y, Yang C, Wu H, Qin J, et al. Solution-processed, undoped, deep-blue organic light-emitting diodes based on starburst oligofluorenes with a planar triphenylamine core. Chem Eur J 2012;18:6928–34.
[34] Cho I, Kim SH, Kim JH, Park S, Park SY. Highly efficient and stable deep-blue emitting anthracene-derived molecular glass for versatile types of non-doped OLED applications. J Mater Chem 2012;22:123–9.
[35] Zheng CJ, Zhao WM, Wang ZQ, Huang D, Ye J, Ou XM, et al. Highly efficient non-doped deep-blue organic light-emitting diodes based on anthracene derivatives. J Mater Chem 2010;20:1560–6.
[36] Han F, Chi LN, Liang XF, Ji SM, Liu SS, Zhou FK, et al. 3,6-Disubstituted carbazole-based bisboronic acids with unusual fluorescence transduction as enantioselective fluorescent chemosensors for tartaric acid. J Org Chem 2009;74:1333–6.
[37] Bloudin N, Leclerc M. Poly(2,7-carbazole)s: structure-property relationships. Acc Chem Res 2008;41:1110–9.

[38] Watanabe M, Nishiyama M, Yamamoto T, Koie Y. Palladium/P(*t*-Bu)$_3$-catalyzed synthesis of *N*-aryl azoles and application to the synthesis of 4,4′,4″-tris(*N*-azolyl)triphenylamines. Tetrahedron Lett 2000;41:481–3.

[39] Adhikari RM, Shah BK, Neckers DC. Photophysical study of blue, green, and orange-red light-emitting carbazoles. J Org Chem 2009;74:3341–9.

[40] Tomkeviciene A, Grazulevicius JV, Kazlauskas K, Gruodis A, Jursenas S, Ke TH, et al. Impact of linking topology on the properties of carbazole trimers and dimers. J Phys Chem C 2011;115:4887–97.

[41] Tsai MH, Lin HW, Su HC, Ke TH, Wu CC, Fang FC, et al. Highly efficient organic blue electrophosphorescent devices based on 3,6-bis(triphenylsilyl)carbazole as the host material. Adv Mater 2006;18:1216–20.

[42] Nakanotani H, Masui K, Nishide J, Shibata T, Adachi C. Promising operational stability of high-efficiency organic light-emitting diodes based on thermally activated delayed fluorescence. Sci Rep 2013;3:2127–31.

[43] Linton KE, Fisher AL, Pearson C, Fox MA, Pålsson LO, Bryce MR, et al. Colour tuning of blue electroluminescence using bipolarcarbazole–oxadiazole molecules in single-active-layer organic light emitting devices (OLEDs). J Mater Chem 2012;22:11816–25.

[44] Sun J, Jiang HJ, Zhang JL, Tao Y, Chen RF. Synthesis and characterization of heteroatom substituted carbazole derivatives: potential host materials for phosphorescent organic light-emitting diodes. New J Chem 2013;37:977–85.

[45] (a) An ZF, Chen RF, Yin J, Xie GH, Shi HF, Tsuboi T, et al. Conjugated asymmetric donor-substituted 1,3,5-triazines: new host materials for blue phosphorescent organic light-emitting diodes. Chem Eur J 2011;17:10871–8;
(b) Tao Y, Xiao J, Zheng C, Zhang Z, Yan M, Chen R, et al. Dynamically adaptive characteristics of resonance variation for selectively enhancing electrical performance of organic semiconductors. Angew Chem Int Ed 2013;52:10491–5;
(c) Han C, Zhang Z, Xu H, Li J, Xie G, Chen R, et al. Controllably tuning excited-state energy in ternary hosts for ultralow-voltage-driven blue electrophosphorescence. Angew Chem Int Ed 2012;51:10104–8;
(d) Yu D, Zhao F, Han C, Xu H, Li J, Zhang Z, et al. Ternary ambipolar phosphine oxide hosts based on indirect linkage for highly efficient blue electrophosphorescence: towards high triplet energy, low driving voltage and stable efficiencies. Adv Mater 2012;24:509–14;
(e) Yang W, Zhang Z, Han C, Zhang Z, Xu H, Yan P, et al. Controlling optoelectronic properties of carbazole–phosphine oxide hosts by short-axis substitution for low-voltage-driving PHOLEDs. Chem Commun 2013;49:2822–4;
(f) Zhang Z, Zhang Z, Chen R, Jia J, Han C, Zheng C, et al. Modulating the optoelectronic properties of large, conjugated, high-energy gap, quaternary phosphine oxide hosts: impact of the triplet-excited-state location. Chem Eur J 2013;19:9549–61.

[46] Miyamoto E, Yamaguchi Y, Yokoyama M. Ionization potential of organic pigment film by atmospheric photoelectron emission analysis. Electrophotography 1989;28:364–70.

[47] Ostrauskaite J, Voska V, Buika G, Gaidelis V, Jankauskas V, Janeczek H, et al. Novel hole-transporting hydrazones. Synth Met 2003;138:457–61.

[48] Thelakkat M, Ostrauskaite J, Leopold A, Bausinger R, Haarer D. Fast and stable photorefractive systems with compatible photoconductors and bifunctional NLO-dyes. J Chem Phys 2002;285:133–47.

[49] Juska G, Nekrasas N, Valentinavicius V, Meredith P, Pivrikas A. Extraction of photogenerated charge carriers by linearly increasing voltage in the case of Langevin recombination. Phys Rev B 2011;84:155202–6.

[50] Juška G, Arlauskas K, Viliūnas M, Kočka J. Extraction current transients: new method of study of charge transport in microcrystalline silicon. Phys Rev Lett 2000;84:4946–54.

[51] de Mello JC, Wittmann HF, Friend RH. An improved experimental determination of external photoluminescence quantum efficiency. Adv Mater 1997;9:230–2.

[52] Harwood LM, Moody CJ. Organic chemistry. Principles and practice. Blackwell Science; 1989.

[53] Hameurlaine A, Dehaen W, Peng H, Xie Z, Tang BZ. Synthesis and light-emitting properties of a new conjugated polymer containing carbazole and quinoxaline moieties. J Macromol Sci Pure Appl Chem 2004;A41:295–303.

[54] Bogdal D, Lukasiewicz M, Pielichowski J. Halogenation of carbazole and other aromatic compounds with hydrohalic acids and hydrogen peroxide under microwave irradiation. Green Chem 2004;6:110–3.

[55] Li Z, Di C, Zhu Z, Li Q, Zeng Q, Zhang K, et al. Structural control of the side-chain chromophores to achieve highly efficient nonlinear optical polyurethanes. Macromolecules 2006;39:6951–61.

[56] Ponce MB, Cabrerizo FM, Bonesi SM, Erra-Balsells R. Synthesis and electronic spectroscopy of bromocarbazoles. Direct bromination of *N*- and *C*-substituted carbazoles by *N*-bromosuccinimide or a *n*-bromosuccinimide/silica gel system. Helv Chim Acta 2006;89:1123–39.

[57] Cabaj J, Idzik K, Sołoduchoand J, Chyla A. Development in synthesis and electrochemical properties of thienyl derivatives of carbazole. Tetrahedron 2006;62:758–64.

[58] Ngbilo E, Ades D, Chevrot C, Siove A. Synthesis and characterization of poly (N-butyl-3,6-carbazolediyl) a new soluble electroactive material. Polym Bull 1990;24:17–22.

[59] Li JC, Meng QB, Kim JS, Lee YSA. Thiophene, benzothiadiazole, and carbazole-based copolymer: synthesis and characterization. Bull Korean Chem Soc 2009;30:951–4.

[60] Zeng Q, Li Z, Dong Y, Di C, Qin A, Hong Y, et al. Fluorescence enhancements of benzene-cored luminophors by restricted intramolecular rotations: AIE and AIEE effects. Chem Commun 2007:70–2.

[61] Sonntag Martin, Kreger Klaus, Hanft Doris, Strohriegl Peter. Novel star-shaped triphenylamine-based molecular glasses and their use in OFETs. Chem Mater 2005;17:3031–9.

[62] del Grosso A, Helm MD, Solomon SA, Caras-Quintero D, Ingleson MJ. Simple inexpensive boron electrophiles for direct arene borylation. Chem Commun 2011;47:12459–61.

[63] Ranger M, Rondeau D, Leclerc M. New well-defined poly(2,7-fluorene) derivatives: photoluminescence and base doping. Macromolecules 1997;30:7686–91.

[64] Kim Jinwoo, Hee KS, Jaehong K, Il K, Youngeup J, Hyun KJ, et al. Diaryl substituted poly(cyclopenta[def]phenanthrene) derivatives containing carbazole and triphenylamine units in the main chain for organic light-emitting diodes. Macromol Res 2011;19:589–98.

[65] Zeng LC, Lee TYH, Merkeland PB, Chen SH. A new class of non-conjugated bipolar hybrid hosts for phosphorescent organic light-emitting diodes. J Mater Chem 2009;19:8772–81.

[66] Gudeika D, Lygaitis R, Mimaitė V, Grazulevicius JV, Jankauskas V, Lapkowski M, et al. Hydrazones containing electron-accepting and electron-donating moieties. Dyes Pigm 2011;91:13–9.

[67] Hodgson HH, Handley FW. LXXIII.—Studies in colour and constitution. Part I. The influence of the methylthiol group, alone and in conjunction with the methoxy-group. Chem Soc 1926:542–6.

[68] Ishow E, Camacho-Aguilera R, Guérin J, Brosseau A, Nakatani K. Spontaneous formation of complex periodic superstructures under high interferential illumination of small-molecule-based photochromic materials. Adv Funct Mater 2009;19:796–804.

[69] Frisch MJ, Trucks GW, Schlegel HB, Scuseria GE, Robb MA, Cheeseman JR, et al. Gaussian 09, revision A.02. Wallingford CT: Gaussian, Inc; 2009.

[70] Gudeika D, Reghu RR, Grazulevicius JV, Buika G, Simokaitiene J, Miasojedovas A, et al. Electron-transporting naphthalimide-substituted derivatives of fluorene. Dyes Pigm 2013;99:895–902.

[71] Jacquemin D, Perpète EA, Scalmani G, Ciofini I, Peltier C, Adamo C. Absorption and emission spectra of 1,8-naphthalimide fluorophores: a PCM-TD-DFT investigation. Chem Phys 2010;372:61–6.

[72] Reghu RR, Grazulevicius JV, Simokaitiene J, Matulaitis T, Miasojedovas A, Kazlauskas K, et al. Glass forming donor-substituted s-triazines: photophysical and electrochemical properties. Dyes Pigm 2013;97:412–22.

[73] Matsubayashi K, Kubo Y. Control of photophysical properties and photoreactions of aromatic imides by use of intermolecular hydrogen bonding. J Org Chem 2008;73:4915–9.

[74] Malinauskas T, Daskeviciene M, Bubniene G, Petrikyte I, Raisys S, Kazlauskas K, et al. Phenylethenyl-substituted triphenylamines: efficient, easily obtainable, and inexpensive hole-transporting materials. Chem Eur J 2013;19:15044–56.

[75] Jursenas S, Kurilcik N, Karpicz R, Gulbinas V, Valkunas L, Rutkis M, et al. Impact of aggregates on excitation dynamics in transparent polymer films doped by dipolar molecules. Thin Solid Films 2008;516:8909–16.

[76] Kersting R, Mollay B, Rusch M, Wenisch J, Leising G, Kauffmann HF. Femtosecond site-selective probing of energy relaxing excitons in poly(-phenylenevinylene): luminescence dynamics and lifetime spectra. J Chem Phys 1997;106:2850.

[77] Katoh R, Suzuki K, Furube A, Kotani M, Tokumaru K. Fluorescence quantum yield of aromatic hydrocarbon crystals. J Phys Chem C 2009;113:2961–5.

[78] Serevicius T, Komskis R, Adomenas P, Adomeniene O, Jankauskas V, Gruodis A, et al. Non-symmetric 9,10-diphenylanthracene-based deep-blue emitters with enhanced charge transport properties. Phys Chem Chem Phys 2014;16:7089–101.

[79] Zotti G, Schiavon G, Zecchin S, Morin JF, Leclerc M. Electrochemical, conductive, and magnetic properties of 2,7-carbazole-based conjugated polymers. Macromolecules 2002;35:2122–8.

[80] Hsiao SH, Liou GYS, Kung YC, Hsiung TJ. Synthesis and properties of new aromatic polyamides with redox-active 2,4-dimethoxytriphenylamine moieties. J Polym Sci A Polym Chem 2010;48:3392–401.

[81] Gudeika D, Michaleviciute A, Grazulevicius JV, Lygaitis R, Grigalevicius S, Jankauskas V, et al. Structure properties relationship of donor–acceptor derivatives of triphenylamine and 1,8-naphthalimide. J Phys Chem C 2012;116:14811–9.

[82] Mozer AJ, Sariciftci NS, Pivrikas A, Österbacka R, Juška G, Brassat L, et al. Charge carrier mobility in regioregular poly(3-hexylthiophene) probed by transient conductivity techniques: a comparative study. Phys Rev B 2005;71:035214–22.

[83] Pivrikas A, Ullah M, Singh TB, Simbrunner C, Matt G, Sitter H, et al. Meyer–Neldel rule for charge carrier transport in fullerene devices: a comparative study. Org Electron 2011;12:161–8.